



Cite this: DOI: 10.1039/d5an01316j

## Exploring the role of microfluidic paper-based analytical devices in salivary diagnostics: from concept to clinical applications

Lucas R. Sousa,<sup>a,b</sup> Larissa G. Velasco,<sup>a</sup> Sandra G. Vlachovsky,<sup>b</sup> Federico Figueredo,<sup>b</sup> Eduardo Cortón<sup>b</sup> and Wendell K. T. Coltro<sup>\*,a,c</sup>

Microfluidic paper-based analytical devices ( $\mu$ PADs) have evolved significantly over the last few decades, from simple colorimetric strips to multifunctional lab-on-a-chip systems. This review focuses on advances in  $\mu$ PAD development, with particular emphasis on their application in salivary diagnostics. It covers the fundamental aspects of these devices, including their fabrication methods, detection strategies (with emphasis on colorimetry and electrochemistry), key biomarkers under investigation, and current challenges. Saliva has emerged as a promising diagnostic fluid due to its non-invasive collection, low risk, and diverse biochemical content, including proteins, enzymes, hormones, and nucleic acids. Salivary diagnostics on  $\mu$ PADs are closely aligned with the WHO's ASSURED criteria, making them highly promising for primary care and resource-limited settings. While some salivary biomarkers are clinically established, many remain understudied and require more accurate screening and comparison with conventional diagnostic methods. Our review also highlights how the remaining challenges, such as biomarker variability, integration of sample pretreatment steps, and interference from biological components, are being resolved by the scientific community. In doing so, we present the state-of-the-art and ongoing advances that are essential to establish  $\mu$ PADs as accessible and effective tools in global public health.

Received 11th December 2025,  
Accepted 24th March 2026

DOI: 10.1039/d5an01316j

rsc.li/analyst

### 1. Introduction

Throughout chordate evolution, salivary glands gradually developed from being absent in fish, rudimentary in amphibians, and more advanced in reptiles to reaching peak complexity in mammals.<sup>1–3</sup> These glands likely evolved from the buccal epithelium through the initial appearance of secretory granules in stratified epithelial tissue. In mammals, saliva composition varies with diet, primarily serving to lubricate food for chewing, capture insects, and facilitate swallowing, as evidenced by the universal presence of mucus-producing cells. Saliva also plays a key role in digestion—primarily through enzymes such as amylase—and contributes to oral health. Its secondary functions include ion transport, secretion of pharmacologically active compounds, reabsorption of blood proteins, and dilution of food. Humans possess three major salivary gland pairs—parotid, submandibular, and sublingual—as

well as numerous minor glands dispersed throughout the oral and upper respiratory mucosa.<sup>4,5</sup>

In humans, 1200 to 1500 mL of saliva is produced every day.<sup>2</sup> The secretion of saliva (salivation) is mediated by parasympathetic stimulation; acetylcholine is the active neurotransmitter and binds to muscarinic receptors in the glands, leading to increased salivation.<sup>6</sup> At the level of the mouth, the saliva produced by all the salivary glands mixes and is combined with different secretions that may be produced by damaged tissue and inflammatory processes occurring at different levels, particularly involving the periodontal tissue. The composition of this complex mixture may be related to various health conditions, so its careful analysis may provide relevant clues about not only oral but also systemic conditions, serving as a strong complement to the analysis of other body fluids.<sup>4,6–9</sup>

#### 1.1 Saliva as a diagnostic fluid

Saliva has been used historically as a diagnostic tool in various cultures and civilizations, including ancient Greece and Rome, in traditional Chinese medicine, and in Ayurvedic medicine, where it provided relevant health indicators referred to at that time as “body imbalances” or “vital energy”. Modern medicine relies primarily on the analysis of blood, urine, and other

<sup>a</sup>Instituto de Química, Universidade Federal de Goiás, 74690-900 Goiânia, GO, Brazil. E-mail: wendell@ufg.br

<sup>b</sup>Departamento de Química Biológica e IQUBICEN–CONICET, Facultad de Ciencias Exactas y Naturales, Universidad de Buenos Aires (UBA), CABA, Argentina

<sup>c</sup>Instituto Nacional de Ciência e Tecnologia de Bioanalítica, 13084-971 Campinas, SP, Brazil

bodily fluids, but recently, the possible value of saliva as a complementary fluid has returned to the table.<sup>2,5,10</sup>

The diagnostic potential of saliva may be relevant due to its non-invasive collection method and comprehensive representation of the body's physiological state. Unlike blood, which requires a needle puncture, saliva can be collected easily, without discomfort, making it a patient-friendly option for frequent monitoring. Additionally, saliva contains biomarkers that reflect both local oral and systemic health conditions, such as hormones, antibodies, nucleic acids, and various metabolites.<sup>11,12</sup>

Salivary diagnostic capabilities extend to the detection of infectious diseases, autoimmune disorders, and even cancers. For instance, the presence of specific viral RNA in saliva can indicate infections such as COVID-19, while elevated levels of certain proteins might signal autoimmune conditions such as Sjögren's syndrome.<sup>13</sup> Salivary diagnostics can also play a crucial role in monitoring metabolic disorders, as changes in the composition of saliva can reflect alterations in the body's metabolic processes.<sup>14,15</sup>

Analysis of saliva can provide insights into an individual's hormone levels, stress markers, and drug consumption, making it a versatile medium for health monitoring. Its potential to reveal systemic conditions by detecting specific biomarkers underscores its value as a diagnostic tool, complementing traditional methods and providing a broader picture of an individual's health.<sup>16</sup>

While saliva diagnostics hold great promise, some challenges need to be addressed to enhance their effectiveness: the main problems are the very low concentrations of potential analytes, the secretion volume and composition related to food or other stimuli, and the need to standardize collection and conservation methods.

## 1.2 Microfluidic paper-based analytical devices ( $\mu$ PADs)

Microfluidic paper-based analytical devices ( $\mu$ PADs) are a cutting-edge advancement in diagnostics and point-of-care (POC) technologies. These devices use paper as a substrate to create microfluidic channels, enabling the manipulation and analysis of small volumes of fluids, such as saliva, blood, or urine.  $\mu$ PADs offer numerous advantages, including low cost, simplicity, portability, and the potential for rapid and accurate diagnostic results.<sup>17,18</sup>

The concept of  $\mu$ PADs emerged from the need for affordable, accessible diagnostic tools for use in resource-limited settings. The development of  $\mu$ PADs was influenced by the principles of microfluidics, which involve precise control and manipulation of fluids at the microscale. Early prototypes of paper-based devices demonstrated the feasibility of using paper to create fluidic pathways, thereby establishing PADs as a distinct technology within the broader field of microfluidics.<sup>19–21</sup>

The design of  $\mu$ PADs involves creating channels and zones on paper through which fluids can flow and react with specific chemicals impregnated into a cellulosic surface. These designs can be achieved through various methods, such as wax print-

ing,<sup>22</sup> inkjet printing,<sup>23</sup> cutting,<sup>24,25</sup> and photolithography.<sup>26</sup> Each method has its advantages and limitations, but wax printing is particularly popular due to its simplicity and cost-effectiveness.

Paper substrates used in the development of  $\mu$ PADs are typically treated to enhance their fluid-handling properties and support the adhesion of reagents. Hydrophobic barriers are usually used to define channels through which fluids can flow, while hydrophilic regions promote fluid transport and reaction. The choice of paper, barrier materials, and fabrication techniques all contribute to the functionality and performance of  $\mu$ PADs.<sup>27,28</sup>

In general,  $\mu$ PADs have demonstrated significant potential in the field of diagnostics, providing a platform for rapid, accurate, and cost-effective detection of various health conditions. Their applications span across, but are not limited to, infectious disease detection, where  $\mu$ PADs can be used to detect pathogens such as bacteria, viruses, and fungi in bodily fluids.<sup>29,30</sup> For instance, during the COVID-19 pandemic,  $\mu$ PADs were developed to detect viral RNA in saliva, offering a non-invasive and rapid diagnostic tool that could be used outside traditional laboratory settings.<sup>31</sup>

Other applications may include the diagnosis of metabolic disorders (*e.g.*, diabetes) by following glucose, ketone bodies, and/or other metabolites, and the detection of biomarkers related to autoimmune or cancer diseases by measuring minute amounts of specific proteins, nucleic acids, or antibodies.<sup>16,18,32</sup>

POC technologies have revolutionized diagnostics by providing immediate results at the point of patient care. These technologies offer a convenient, rapid, and cost-effective approach to disease detection, monitoring, and management.<sup>4,32</sup> POC diagnostics are designed for use in various settings, including hospitals, clinics, and even remote locations, making healthcare more accessible and efficient. The development of innovative diagnostic tools, such as  $\mu$ PADs, has further enhanced the capabilities of POC technologies.<sup>10</sup>

One of the most significant advantages of  $\mu$ PADs is their suitability for POC technologies, allowing immediate testing and results at the point of patient care, bypassing the need for centralized laboratories and long wait times.  $\mu$ PADs can be integrated into POC systems to provide rapid diagnostic results, which are essential for timely medical decision-making and treatment.<sup>33</sup>

Paper-based devices represent a transformative advancement in diagnostic technology, offering a low-cost, portable, and efficient means of detecting a variety of health conditions. Their potential to revolutionize POC diagnostics and deliver accessible healthcare solutions across diverse settings underscores their importance in the future of medical science.<sup>34</sup> As research and technology continue to evolve,  $\mu$ PADs are poised to become an integral part of the global healthcare landscape, enabling rapid and accurate diagnostics that can save lives and improve health outcomes worldwide. Future research and development should focus on addressing current limitations

and expanding  $\mu$ PAD capabilities. Innovations in material science, microfluidic design, and data integration will drive the evolution of paper-based platforms, making them more robust and versatile for a wide range of diagnostic applications.<sup>33</sup>

Based on this scenario, this review presents an updated and comprehensive overview of the role of saliva as a diagnostic fluid, with a focus on its integration into paper-based microfluidic devices. Considering the evolutionary, physiological, and biochemical significance of saliva, this review explores how its complex composition can reflect both local and systemic health conditions. By analyzing current advances in  $\mu$ PAD technology and its synergy with POC diagnostic approaches, we aim to highlight the potential of these innovative tools for facilitating accessible, non-invasive, and cost-effective health monitoring. Special attention is given to recent advances in  $\mu$ PAD fabrication and detection approaches coupled with salivary diagnostics.

Despite the well-established diagnostic relevance of saliva, its routine clinical application still relies largely on centralized laboratory techniques such as enzyme-linked immunosorbent assays (ELISA), high-performance liquid chromatography (HPLC), liquid chromatography–mass spectrometry (LC–MS/MS), and reverse transcription polymerase chain reaction (RT-PCR) analyses.<sup>2,9,16</sup> While these methods provide high analytical sensitivity and specificity, they require sophisticated instrumentation, trained personnel, controlled laboratory environments, and multi-step sample preparation, often associated with increased cost and turnaround time. As a result, a disconnect persists between the non-invasive nature of saliva as a diagnostic fluid and its practical implementation in point-of-care settings.

In parallel, significant advances have been achieved in the development of paper-based platforms for salivary diagnostics. However, the field remains heterogeneous, encompassing diverse fabrication strategies, detection modalities, and levels of clinical validation, making it unclear how current efforts converge toward robust and scalable solutions. This review addresses this need by providing a critical summary of the integration between salivary diagnostics and microfluidic paper-based analytical devices ( $\mu$ PADs), examining technological progress alongside analytical performance, validation status, and translational prospects.

## 2. Paper as substrate

Paper has been used as a substrate for various purposes in biotechnology and biochemistry due to its unique properties, such as biocompatibility, accessible manufacturing, adjustable porosity, eco-friendly, and global affordability. Eventually, these unique properties, particularly their absorptive and capillary transport capacity, began to be explored more systematically, particularly for health-related applications.<sup>28,35,36</sup>

An innovative report on the use of this substrate as an analytical device was published in 2007 when the group of George M. Whitesides introduced the first example of a

$\mu$ PAD.<sup>37</sup> In this remarkable report, the authors used standard photolithography to create microchannels delimited by hydrophobic barriers, allowing spontaneous fluid flow transport without pumps or mechanical systems. This pioneering work established  $\mu$ PADs and PADs as innovative platforms for POC clinical diagnostics, initially focused on blood sample analysis.

Since then,  $\mu$ PADs have emerged as ingenious systems capable of manipulating small volumes of liquid by capillary action, eliminating the need for pumps or external power sources. These devices enable localized chemical reactions and efficient transport of samples and reagents, enabling integration with conventional bioanalytical techniques, such as extraction/separation processes, purification methods, and various detection strategies.<sup>38</sup> Although colorimetry remains the most commonly used detection technique coupled with these devices, electrochemical protocols, fluorescence applications, and even paper spray ionization coupled with mass spectrometry have expanded the application possibilities and analytical sensitivity.<sup>18</sup>

Initially used for the detection of biomarkers in blood,<sup>39</sup>  $\mu$ PADs soon showed potential for other biological matrices. In particular, saliva stood out as a promising sample due to its non-invasive collection and the relevant diagnostic information it contains. Blicharz *et al.* and Nagler were among the pioneers in the use of paper strips for colorimetric testing of saliva, focusing on biomarkers such as nitrite and uric acid, particularly in clinical settings, including patients with end-stage renal disease.<sup>9,40</sup> These studies demonstrated the feasibility of simple and affordable devices for non-invasive monitoring of biomarkers in saliva. Their report, although not presented in the context of  $\mu$ PADs, was a milestone for the development of PADs for saliva analysis in subsequent studies.

Since then, several studies have expanded the scope of saliva analysis using  $\mu$ PADs, enabling practical, accessible monitoring of infectious, metabolic, and even neurological diseases.<sup>41</sup> In addition to human health,  $\mu$ PADs have been widely explored in other fields such as environmental monitoring,<sup>42</sup> petrochemistry,<sup>43</sup> forensic science,<sup>44</sup> and food quality control<sup>45</sup> due to their simplicity, low cost, and portability.

### 2.1 Manufacturing considerations for paper-based saliva diagnostics devices

The fabrication of  $\mu$ PADs has progressed since the pioneering report demonstrated the use of photolithography to create microfluidic pathways on paper. Nowadays, new methods such as wax printing,<sup>37</sup> laser ablation,<sup>20</sup> inkjet printing,<sup>27</sup> and screen printing<sup>46</sup> have been introduced, allowing for more versatile, accessible and scalable designs. These approaches have evolved to improve fluid control, enhance analytical performance and facilitate integration with detection systems.<sup>37</sup> Given the intrinsic advantages, paper-based platforms have become particularly attractive for POC diagnostics, especially in saliva-based applications.

As shown in Fig. 1, the process for establishing a protocol for saliva analysis and diagnosis involves several key steps,

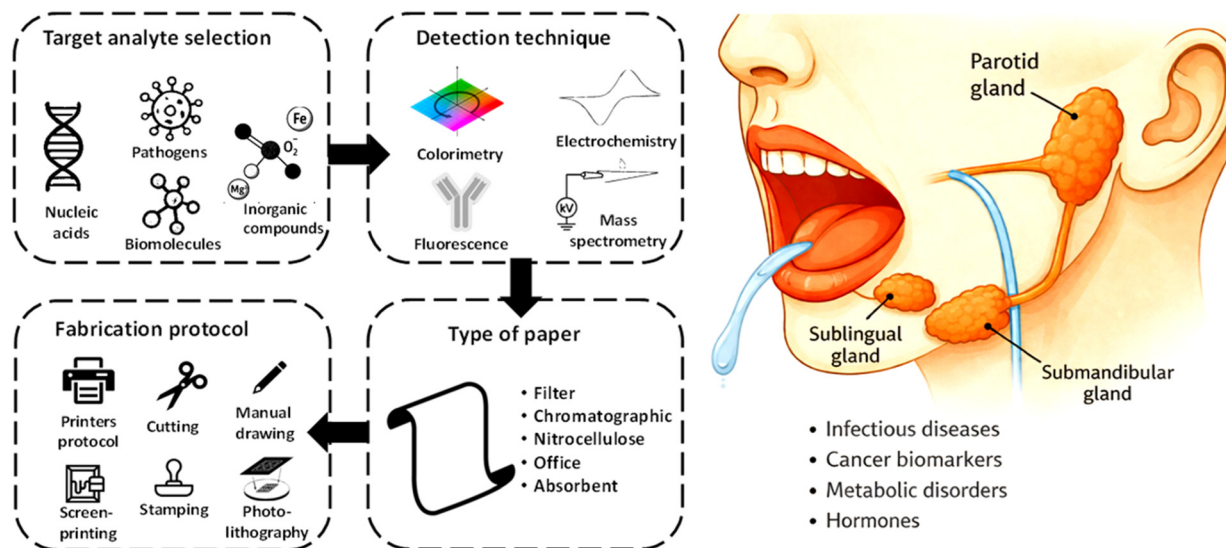


**Fig. 1** Illustration showing the saliva production pathway—an important fluid that reflects patients' health and clinical status—originating from the salivary glands and how an analysis protocol using PADs can be designed for this substrate. The protocol may vary depending on the target analyte: the most suitable detection method is selected based on the analyte's chemical properties, followed by the choice of paper type that supports the detection technique and serves as a reservoir for saliva handling, and finally, a fabrication method is tailored as per user convenience.

including the selection of the target analyte, the detection method, and the most appropriate paper type for optimal resolution. Saliva is a particularly suitable biological fluid for  $\mu$ PAD applications due to its physicochemical properties, particularly its viscosity, which ranges from approximately 1.0 to 3.0 mPa s, depending on hydration and stimulation conditions. This is close to the viscosity of water (approximately 0.89 mPa s at 25 °C) and allows predictable and uniform capillary flow in porous substrates.<sup>46</sup> As a result, saliva is compatible with virtually all existing  $\mu$ PAD fabrication techniques, including both high- and low-resolution patterning methods. As a result, the choice of fabrication strategy for saliva-based diagnostics is often determined not by fluid compatibility, but by other practical considerations such as production cost, equipment availability and suitability for use in remote or resource-limited settings.

Despite the diversity of fabrication approaches, batch-to-batch variability remains a non-negligible issue. Differences in paper porosity, fiber distribution, surface treatments, and manual reagent deposition can lead to fluctuations in capillary flow rates and analytical responses. Such variability becomes particularly critical when quantitative readouts are required, highlighting the need for standardized manufacturing workflows and quality control protocols. In response to these issues, the choice of the substrate type is critical for constructing an effective salivary sensor and should be the first consideration when accounting for the requirements of the detection technique and the analytical steps involved.

**2.1.1 Paper selection.** The type of paper plays an important role in the fabrication of paper-based devices, and must be defined prior to the fabrication step based on the intended

application of the device.<sup>47–49</sup> In diagnostic applications, the type of analytical technique to be used in the device is the primary factor that determines the selection of both the fabrication method and the paper substrate, as these will dictate the fluidic behavior, sensitivity, and overall analytical performance of the device.

There are several types of paper used in the fabrication of  $\mu$ PADs, each with specific properties that directly influence the performance of diagnostic tests. The most commonly used papers for the manufacture of paper-based analytical devices include chromatography paper,<sup>50–52</sup> office paper,<sup>53,54</sup> qualitative filter paper,<sup>41</sup> vegetal paper,<sup>55</sup> absorbent paper and nitrocellulose membranes.<sup>56,57</sup> Fig. 2 presents key examples from the literature of different  $\mu$ PAD formats developed on various paper types, all applied to saliva analysis. Chromatography paper and filter paper were the first paper substrates chosen for saliva analysis. Chromatographic paper—particularly Whatman® Grade 1—is widely used because of its uniform porosity, good reagent retention capacity and consistent capillary flow. Chromatography paper provides excellent resolution for separations and is ideal for assays involving multiple reaction zones.<sup>58</sup> Office paper has been explored as an inexpensive and widely available alternative, particularly in applications where high precision in liquid flow is not required. Absorbent paper is often used in lateral flow assays due to its high liquid absorption capacity and ability to hold large volumes of sample.<sup>54</sup> Nitrocellulose membranes, on the other hand, are particularly valued in immunoassays for their strong protein-binding properties and fast capillary action. The correct choice of paper type is important to ensure the sensitivity, selectivity and reproducibility of paper-based instruments, particularly in clinical diagnostic applications.<sup>19,59,60</sup>

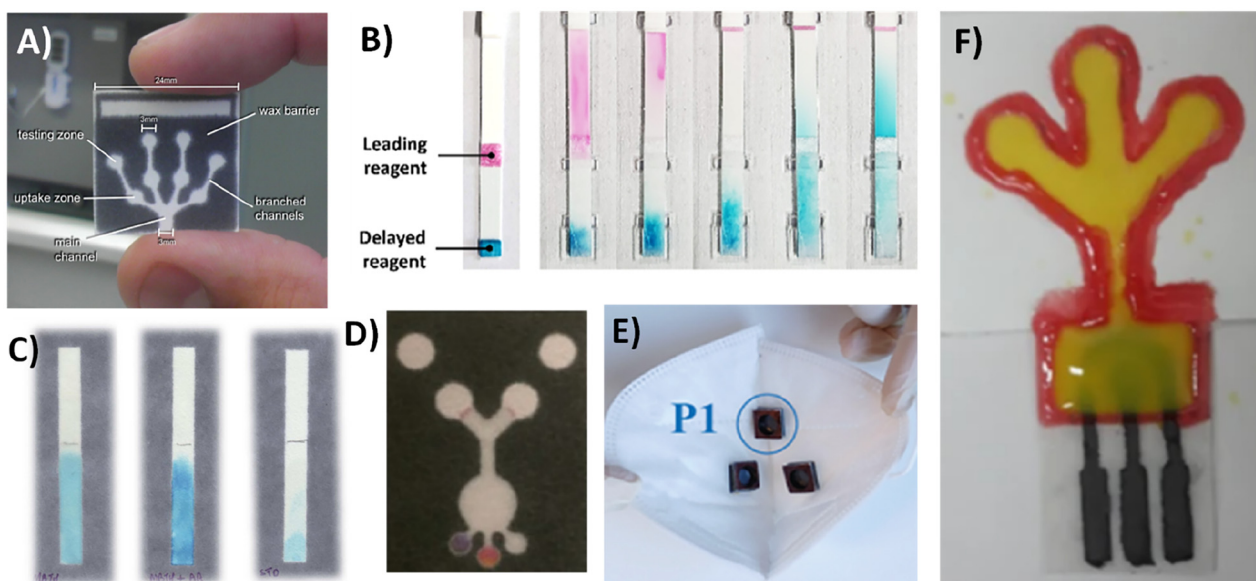


**Fig. 2** Representation of different paper-based analytical devices using chromatographic paper (A), nitrocellulose (B), absorbent paper (C), qualitative filter paper (D), office paper (E), and a combination of chromatographic paper (top side) and parchment paper (bottom side) (F) for the construction of sensors for clinical analysis in saliva samples. Images A, B, C, D, E and F were reprinted with permission from the references Bhakta *et al.*,<sup>61</sup> Kim and Kim,<sup>66</sup> Ramdzan *et al.*,<sup>191</sup> Noiphung *et al.*,<sup>100</sup> Gutiérrez-Gálvez *et al.*<sup>69</sup> and Sousa *et al.*,<sup>55</sup> respectively.

Although paper selection is often guided by analytical compatibility, limited reporting on inter-lot reproducibility and long-term storage stability of functionalized substrates still represents a gap in the literature. In clinical settings, even minor variations in wicking speed or protein-binding capacity may compromise quantitative accuracy and comparability between devices.

In the context of salivary diagnostics, papers with high absorption capacity and controlled porosity are preferred to ensure efficient sample transport and interaction with reagents. One of the pioneering works using  $\mu$ PADs for salivary diagnostics was performed by Bhaktha *et al.*, who developed a colorimetric device for nitrite detection in saliva, as shown in Fig. 2A. In their study, the authors used Whatman Grade 1 chromatographic paper, chosen for its favorable wicking properties and compatibility with the colorimetric detection method based on a modified Griess reaction. The devices were designed to quantify nitrite levels, a potential marker for periodontitis, and demonstrated sensitivity and limits of detection (LOD) suitable for real sample analysis.<sup>61</sup>

However, for examples of applications requiring specific biomolecular interactions, such as immunoassays, nitrocellulose membranes are often preferred. While nitrocellulose is more porous than chromatographic paper due to its three-dimensional fibrous network and high adsorption capacity (especially for proteins and nucleic acids), it is less permeable to capillary flow due to its smaller pore size and denser structure.<sup>62,63</sup> This difference in permeability has a direct impact on instrument design and assay performance, especially when controlling flow rate and maximizing reaction time are critical.<sup>64</sup>

This effect often dictates the use of nitrocellulose instead of chromatographic paper, especially for immunoassays. For example, Choi *et al.* developed a lateral flow immunoassay (LFA) using a photoluminescent film for the detection of salivary cortisol.<sup>65</sup> This assay achieved high sensitivity through smartphone-based photoluminescence detection and machine-learning algorithms for data analysis, providing accurate cortisol measurements in human saliva samples without the need for an external light source.

Similarly, Kim and Kim proposed an automatic signal-enhanced lateral flow immunoassay (asLFI), represented in Fig. 2B, that significantly improved colorimetric sensitivity for cortisol detection in saliva, achieving a LOD of  $3.8 \text{ pg mL}^{-1}$  with strong correlation to ELISA results.<sup>66</sup> Therefore, nitrocellulose remains the standard material for LFA and is still widely used in saliva-based diagnostics due to its high protein-binding capacity, which enables reliable immobilization of antibodies and antigens. These properties are critical in immunodiagnostics, where specific antigen-antibody interactions must occur in confined zones without dispersion.<sup>67</sup>

Qualitative filter paper, with its high porosity, allows for the separation of solids from saliva, while absorbent paper facilitates the collection and distribution of liquids, which is essential for the controlled movement of samples in microfluidic devices. Although not as widely reported as chromatographic paper, the value of these materials lies in their ability to significantly reduce the final cost of the device. Fig. 2C and D illustrate examples of salivary analysis devices using absorbent paper and viscosity control using qualitative filter paper, respectively.<sup>68</sup>

Office paper has also been used as a viable option for saliva analysis because its properties are similar to those of chromatographic paper, but with lower hydrophilicity, allowing substances to accumulate more easily on its surface. Gutiérrez-Gálvez *et al.* explored this concept by integrating an office paper-based collector into an N95 mask for detecting SARS-CoV-2 spike proteins in exhaled breath, as shown in Fig. 2E.<sup>69</sup> The approach, using a magnetic bead-based electrochemical immunosensor, demonstrated high sensitivity and selectivity, enabling accurate biomarker detection without the need for chemical reagents. This study highlights the potential of paper as a collecting material, showcasing its application in rapid and accessible diagnostic tools for respiratory diseases.

An alternative way of combining the advantages of different types of paper was reported by Sousa *et al.*, who described a manual fabrication protocol for a colorimetric module that achieved higher resolution on chromatographic paper.<sup>55</sup> This was combined with parchment paper on which conductive paths were defined using a screen-printing technique. Fig. 2F shows the final device, in which the two modules were integrated using a photocurable resin.

**2.1.2 Surface treatments.** Surface treatments are often used to optimize paper for specific applications. Recent studies have explored chemical and structural modifications of the paper surface to improve analytical performance. Chitosan is particularly attractive for paper modification in  $\mu$ PADs due to its biocompatibility, film-forming ability, and the presence of amino groups that enhance surface functionality and analyte interaction.<sup>70</sup> For example, Castro *et al.* enhanced the uniformity of color to detect glucose and nitrite in saliva samples by modifying the surface with chitosan, thereby improving the sensitivity and reliability of the colorimetric measurements.<sup>71</sup> Similarly, Chi *et al.* designed a biodegradable fluidic device capable of efficient saliva sampling and salivary biomarker detection. Their device utilized a chitosan sponge for saliva collection and an enzyme-entrapped hydrogel for enhanced colorimetric detection of biomarkers such as glucose and creatinine, demonstrating its potential for POC diagnostics.<sup>72</sup>

Functionalization of nanoparticles, especially with gold or silver nanoparticles, has been shown to enhance colorimetric detection, improving the sensitivity of electrochemical and colorimetric detection and even enabling enzyme-free assays.<sup>73,74</sup> Gold nanoparticles (AuNPs) have been employed as peroxidase-like nanozymes to facilitate glucose monitoring in paper-based devices, providing rapid and reliable colorimetric readouts.<sup>74</sup>

Although still recent, oxidative treatments using sodium periodate have also been reported to introduce aldehyde groups on the cellulose surface, allowing subsequent covalent coupling of antibodies and other biorecognition elements for increased assay stability and selectivity. In addition, plasma treatment remains a versatile method for increasing surface energy and improving wettability, and is often used as a pre-treatment step to facilitate further functionalization.<sup>75</sup> These surface strategies are particularly valuable in saliva-based diagnostics, where low analyte concentrations and matrix interfer-

ences require enhanced selectivity, strong analyte retention and controlled microfluidic behavior to ensure accurate and reproducible results.

However, many surface modification strategies, particularly those involving nanoparticles or enzyme immobilization, may compromise long-term stability under non-controlled storage conditions. Humidity, oxidation, and gradual loss of bioactivity can significantly reduce shelf-life, which remains insufficiently addressed in most proof-of-concept studies. Therefore, future developments should prioritize stabilization strategies, such as protective coatings, incorporation of stabilizing agents, optimized packaging, and systematic shelf-life validation, to ensure practical applicability and real-world robustness of surface-modified  $\mu$ PADs.

**2.1.3 Fabrication strategies.** The fabrication of paper-based analytical platforms has evolved significantly, moving from more complex methods to simpler, cost-effective techniques that promote scalability and mass production of these devices, including in the POC setting. The pioneering study by the Whitesides group used photolithography and chromatographic paper, but the initial choice of fabrication techniques has since moved towards more accessible and efficient methods, with an increasing focus on new tools and, as mentioned, alternative paper substrates,<sup>37</sup> each offering unique advantages depending on the intended application.

*Printing methods.* Printing techniques are among the most widely used methods for the fabrication of paper-based devices due to their versatility, low cost, and scalability. Several different printing methods have been explored to produce  $\mu$ PADs, each with its own advantages and disadvantages. Wax printing is one of the best-known; in this approach, wax is deposited on paper substrates, which can be melted to create hydrophobic barriers, as represented in Fig. 3A.<sup>22,76</sup> Over the years, this technique, which can create stable hydrophobic barriers, has proven to be very affordable and suitable for high-throughput applications. The main problem with this manufacturing method is that laser printing machines are no longer in use, as they have been discontinued.

As a result, other manufacturing methods associated with printing have gained popularity and can be explored through saliva analysis. Laser printing, which offers precise control over material deposition, allows the direct modification of paper to create efficient hydrophobic barriers.<sup>54,77,78</sup>

Inkjet printing, which uses commercial or custom-formulated inks to create patterns on paper, is versatile and widely available.<sup>23</sup> Beyond defining hydrophobic barriers, inkjet technology enables the precise deposition of bio-inks containing enzymes, antibodies, nanoparticles, or redox mediators directly onto specific detection zones. This digital and mask-free approach allows controlled reagent loading, reduced material consumption, and improved spatial resolution. Recent advances in printable bio-ink formulations have enhanced biomolecule stability and minimized nozzle clogging, thereby improving reproducibility and scalability in  $\mu$ PAD fabrication.<sup>79–82</sup>

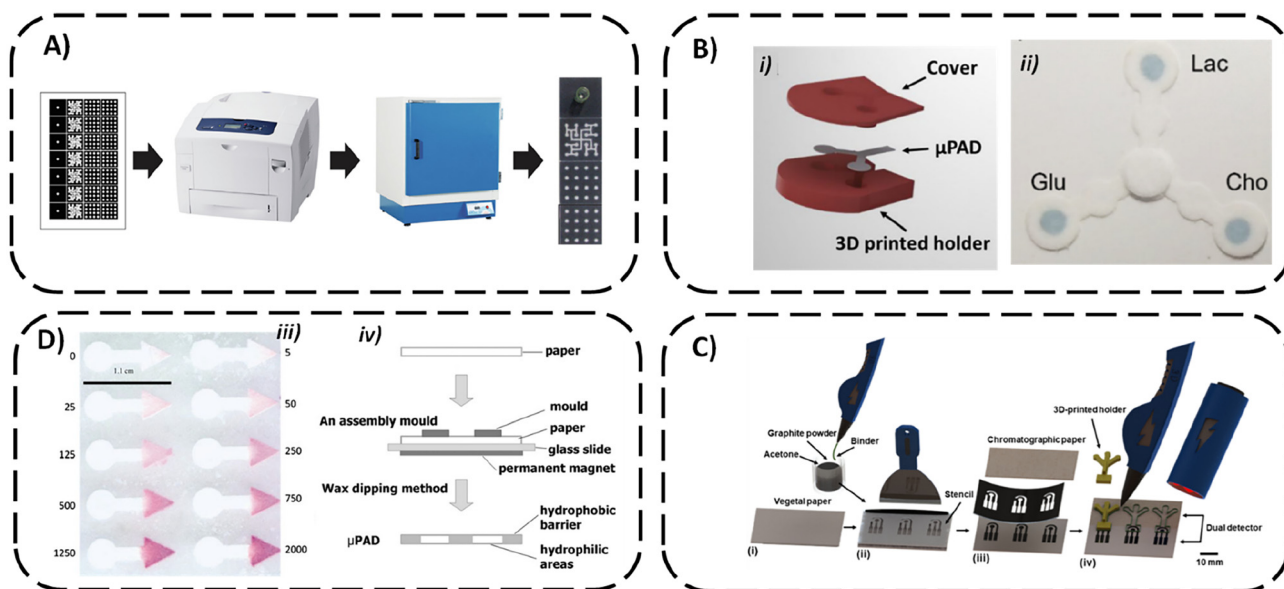


**Fig. 3** Representative examples of the fabrication techniques for the microfluidic paper-based analytical devices ( $\mu$ PADs) used in salivary analysis. (A) Wax printing: hydrophobic barriers formed by wax deposition and melting onto paper substrates. (B-i) Manual paper cutting using craft tools for defining the microfluidic zones and (B-ii) laser cutting and engraving for precise micro-structuring of the paper to enhance fluidic control and create complex channels. (C) Combination of manual drawing with a 3D pen to define the hydrophobic zones and screen-printing with carbon-based ink to form conductive electrodes for dual-mode detection. (D-i) Photolithographic fabrication using UV light and photoresist-coated paper to generate high-resolution microfluidic patterns and (D-ii) wax dipping technique, where molten wax is transferred to the paper using a laser-cut mold to rapidly form the hydrophobic barriers. Images A, B, C, and D were reprinted, with permission, from Rossini *et al.*,<sup>188</sup> de Castro *et al.*,<sup>71</sup> Pomili *et al.*,<sup>85</sup> Klasner *et al.*,<sup>92</sup> Songjaroen *et al.*,<sup>76</sup> and Sousa *et al.*,<sup>55</sup> respectively.

Liang *et al.* demonstrated, for example, a low-cost reagent spraying method using a modified commercial inkjet printer for AST and ALT assays, highlighting scalability and reproducibility. Advances in inkjet-based bioprinting have deepened the understanding of bio-ink formulation, droplet dynamics, shear-induced stress, and substrate–droplet interactions.<sup>82</sup> Optimization of cell or biomolecule homogeneity and droplet impact behavior plays a critical role in ensuring uniform deposition and functional stability. Although primarily developed for tissue engineering, these insights are directly applicable to  $\mu$ PAD fabrication, where reagent distribution homogeneity and deposition precision strongly influence analytical reproducibility and device performance.<sup>82</sup>

3D plotting printers, although still in their infancy, can print functional materials or structural elements onto paper substrates to create more complex, three-dimensional devices.<sup>23,83</sup> Espinosa *et al.* demonstrated this approach by integrating 3D printing with wax filaments to fabricate hydrophobic channels on paper substrates.<sup>83</sup>

One of the most recent printing strategies is thermal transfer printing, which uses heat to transfer ink from a ribbon to a paper substrate and is commonly used to create precise patterns and designs. It has been explored for the creation of hydrophobic barriers in paper-based assays, as shown by Monju *et al.*, with recent advances in the use of this technique for improved pattern fidelity and device performance.<sup>84</sup> Each of these printing methods offers unique advantages, making

them valuable for the fabrication of PADs, including applications in salivary diagnostics.

**Cutting and engraving techniques.** Cutting techniques are essential for shaping paper-based substrates into the required shape for  $\mu$ PADs without the need for a hydrophobic barrier of any material, thus eliminating chemical compatibility issues. Both artisanal (Fig. 3B-i) and laser-based (Fig. 3B-ii) methods provide a variety of options for customizing the device shapes used in cutting protocols.<sup>85,86</sup> Laser engraving enables precise micro-structuring of paper substrates and is particularly suited for the fabrication of intricate designs required in complex  $\mu$ PAD architectures. Pungjunun *et al.* demonstrated the application of laser-engraved hollow microcapillary channels to construct a paper-based microfluidic device capable of dual-mode detection—colorimetric and electrochemical—for salivary biomarkers.<sup>87</sup> Their device, designed specifically to handle viscous samples such as human saliva, uses laser-micropatterned capillary grooves that act as micropumps, enhancing fluid transport without the need for external instrumentation. This approach exemplifies the potential of laser-based fabrication methods for the development of saliva diagnostics, offering low-cost, portable, and sample-efficient alternatives for detecting analytes, such as thiocyanate, with high sensitivity and reliability.

Craft cutter-based patterning, such as that performed using the Silhouette Studio platform, remains a relevant and accessible approach for the development of paper-based microfluidic

devices, especially in resource-limited settings.<sup>86</sup> These manually patterned devices include distinct detection zones connected by microfluidic channels and have been successfully validated with real human saliva samples, showing results comparable to those of spectrophotometric analysis.

Beyond conventional engraving, laser ablation enables more refined microstructural control over paper substrates. By adjusting the laser wavelength and power, it is possible to not only define channel geometry but also locally tune paper thickness, porosity, and surface chemistry, thereby influencing capillary pressure and fluid transport. Recent studies have demonstrated that controlled laser processing can modify the cellulose network while preserving mechanical integrity, directly impacting wicking behavior and sensing performance.<sup>27,31,88</sup> For example, Zhao *et al.* reported laser-induced surface functionalization that enhanced chemical reactivity and fluid manipulation in paper-based platforms. Such advances illustrate how laser-ablated microstructures extend beyond shaping techniques to become powerful tools for enhanced fluidic regulation in  $\mu$ PADs.<sup>88</sup>

**Manual strategies.** Manual protocols are basic techniques that use simple methods such as stamping, screen printing and hand drawing to produce paper-based devices. These methods require minimal equipment, making them particularly suitable for low-cost development and early-stage applications. Stamping involves pressing a patterned mold onto the paper substrate to create the desired shapes or barriers.<sup>89</sup> This technique has been used in the early stages of saliva diagnostic device development, where simple patterning is sufficient for basic functionality. Screen printing is a well-established technique for fabricating  $\mu$ PADs, enabling the precise deposition of hydrophobic materials onto paper substrates using mesh screens. This method is particularly advantageous for mass production due to its reproducibility and low cost. Sitanurak *et al.* demonstrated the use of PVC-based t-shirt ink to produce hydrophobic barriers with high resolution ( $486 \pm 14 \mu\text{m}$ ) and excellent chemical resistance, suitable for the colorimetric detection of analytes, such as nitrite and thiocyanate, in saliva.<sup>90</sup> More recently, Silva-Neto *et al.* employed a stencil-printing approach using glass varnish as the hydrophobic agent to fabricate  $\mu$ PADs for the detection of salivary  $\alpha$ -amylase, achieving reliable microfluidic performance and successful application in real saliva samples.<sup>91</sup>

Manual drawing represents an accessible and low-cost method for fabricating paper-based microfluidic devices, where hydrophobic barriers and functional zones are created directly on paper substrates using pens or markers. A remarkable example is the use of a 3D pen, as reported by Sousa *et al.*, who demonstrated the feasibility of creating  $\mu$ PADs by manually drawing patterns with an acrylate-based resin followed by UV curing. Despite its simplicity, the technique proved effective for both clinical and environmental applications, including salivary diagnostics. The instrument-free nature and affordability of this method make it especially attractive for rapid prototyping and implementation in any place.<sup>55</sup> A representation of manual drawing combined with screen-printing protocol is shown in Fig. 3C.

By combining manual drawing techniques with screen-printing approaches, the authors demonstrated a versatile “do-it-yourself” (DIY) protocol for the fabrication of dual-detection paper-based analytical devices (dual- $\mu$ PADs). Using a 3D pen to draw hydrophobic barriers and a stencil-printing method with carbon-based ink to produce conductive electrodes, the authors successfully developed  $\mu$ PADs capable of simultaneous colorimetric and electrochemical detection. This strategy enabled analysis of salivary biomarkers such as nitrite, lactate, pH, and  $\alpha$ -amylase without the need for sophisticated instrumentation, reinforcing the potential of low-cost fabrication methods for point-of-care diagnostics, especially in periodontal disease screening.<sup>55</sup>

**Photolithography.** Photolithography is a high-precision method that has traditionally been used to fabricate micro-devices in other types of substrates, such as glass. This technique has found applications in paper-based microfluidic devices because it can be used to create high-resolution patterns<sup>37</sup> due to the use of ultraviolet (UV) light to expose a photoresist-coated surface, allowing selective removal of material and the creation of micro-scale channels. The precision of photolithography makes it particularly suitable for applications requiring highly defined flow patterns, such as diagnostic applications.

Klasner *et al.* demonstrated the fabrication of  $\mu$ PADs using photolithography, where devices were fabricated in under 3 min and were immediately ready for use in colorimetric assays for urinary ketones, glucose, and salivary nitrite (see Fig. 3D-i).<sup>92</sup> These devices provided semi-quantitative results for clinically relevant biological assays, proving the potential of photolithography for fast and accessible diagnostic applications. However, the high cost of this technique and its high material, skilled labor and cleanroom requirements have made it unattractive for point-of-care diagnostics. Although photolithography-based device models should be considered for the advancement of other types of manufacturing methods, the technique has not been used for its purpose in  $\mu$ PADs and diagnostics, including saliva.

**Other techniques.** Several techniques, often used in combination, have also emerged for manufacturing  $\mu$ PADs, each offering unique advantages for salivary diagnostic applications. Flexography is a printing process that uses flexible plates to transfer ink onto paper and is suitable for large-scale production of paper-based devices. Recent studies have explored its potential for high-volume production of diagnostic devices, offering a scalable and efficient approach.<sup>93</sup>

Wax dipping, a simple and cost-effective technique, involves immersing paper substrates into molten wax to create hydrophobic barriers. This method has gained popularity in the fabrication of  $\mu$ PADs due to its affordability and ease of implementation.<sup>76</sup> Songjaroen *et al.* introduced a novel wax-dipping approach for producing  $\mu$ PADs utilizing an iron mold created *via* laser cutting to transfer patterns onto the paper (see Fig. 3D-ii). The process is quick, requiring only 1 min to be concluded without the need for complicated instruments or organic solvents. The hydrophobic barriers created *via* this

method have been shown to effectively support clinical diagnostic applications, including glucose and protein detection.<sup>76</sup>

### 3. Operating principles of saliva analysis in paper-based devices

Paper-based analytical devices, in particular  $\mu$ PADs, typically operate by incorporating hydrophilic areas delimited by hydrophobic barriers that enable precise fluid handling. Two-dimensional  $\mu$ PADs (2D- $\mu$ PADs) feature microfluidic structures arranged within a single planar surface, where channels direct fluid movement under capillary forces.<sup>94–96</sup> These devices rely on capillary action for fluid transport, governed primarily by the Lucas-Washburn equation as follows (eqn (1)):

$$L(t) = \left( \frac{\gamma D \cos \theta}{2\mu} \right)^{1/2} \times t^{1/2}, \quad (1)$$

where  $L(t)$  is the distance traveled by the liquid front over time  $t$ ,  $\gamma$  is the surface tension,  $D$  is the effective pore diameter of the paper,  $\theta$  is the contact angle, and  $\mu$  is the dynamic viscosity of the fluid.

This equation highlights the inverse relationship between viscosity and flow rate in porous substrates, an important consideration when working with biological fluids.<sup>97–99</sup> In the case of saliva, its non-Newtonian nature and higher viscosity, resulting from proteins such as mucins and other macromolecules naturally present in its composition, can reduce the rate and uniformity of fluid migration across the paper matrix.<sup>100</sup> Such behavior requires careful adjustment of design parameters such as paper thickness, pore size, and channel geometry. For instance, thicker papers or those with tightly packed fibers increase hydraulic resistance, as can be described by Darcy's law, represented in eqn (2) as follows:

$$Q = \frac{kA\Delta P}{\mu L}, \quad (2)$$

where  $Q$  is the volumetric flow rate,  $k$  is the permeability of the paper,  $A$  is the cross-sectional area,  $\Delta P$  is the pressure difference (often negligible in DAPs),  $\mu$  is the viscosity, and  $L$  is the flow path length. Even under capillary conditions, a higher viscosity ( $\mu$ ) significantly decreases the flow rate.

One approach to overcome the possible effects of salivary viscosity on paper devices is appropriate sample treatment. Several studies have reported the use of filter paper to enable self-sampling and sample pre-treatment of saliva, taking advantage of its intrinsic filtration properties.<sup>99</sup> However, other approaches describe the use of alternative filtration materials to minimize biofouling effects.<sup>96</sup>

An effective approach to circumvent the effects of saliva viscosity in paper-based devices was proposed by Noiphung *et al.*<sup>100</sup> In their study, the authors demonstrated that the addition of a simple buffer washing step after sample application allows the analytical response to be stabilized in colorimetric assays for pH and nitrite, regardless of the initial vis-

cosity of the fluid.<sup>100</sup> This strategy enables consistent and reproducible calibration curves to be obtained even in samples with artificial viscosity ranging from 1.54 to 5.10 mPa s, bringing the performance of the  $\mu$ PAD closer to that of standard methods, without the need for complex treatments or dilutions. In addition to controlling the matrix itself, adjustments in channel width can also optimize flow dynamics. Wider channels facilitate the movement of viscous samples such as saliva, while narrower ones enhance capillary action for low-viscosity fluids.<sup>49</sup> Additionally, gradual tapering or expansion of channels can be used strategically to regulate flow and improve reagent interaction zones.

Beyond intrinsic viscosity differences, pre-analytical variables associated with saliva collection, such as stimulated *versus* unstimulated saliva, circadian variations, hydration status, and recent food intake, can significantly modify both the viscosity and surface interaction properties of the sample. These variations directly impact the parameters described in the Lucas-Washburn and Darcy models, altering capillary flow distance and volumetric flow rate within the  $\mu$ PAD channels.<sup>101,102</sup> Consequently, inconsistencies in sample collection may translate into variations in fluid migration kinetics, reagent interaction time, and ultimately analytical signal intensity. Therefore, standardization of saliva collection protocols and incorporation of design strategies that compensate for matrix variability are essential to ensure reproducibility and reliable clinical performance of saliva-based  $\mu$ PADs.

#### 3.1 Three-dimensional paper-based microfluidic devices

The use of three-dimensional  $\mu$ PADs (3D- $\mu$ PADs) has proven particularly advantageous for the analysis of complex samples such as saliva. These devices allow vertical and horizontal paths for the fluid, enabling the integration of different analytical steps in overlapping layers of paper. In contrast to two-dimensional devices, 3D- $\mu$ PADs allow more elaborate configurations, allowing fluid to flow in both lateral and vertical directions between multiple layers of paper. This architecture favors the creation of multiple detection zones, allowing simultaneous and rapid quantification of different analytes.<sup>94–96,103</sup> Although more commonly used for more complex biological matrices such as blood, these devices can also be a viable alternative for saliva analysis, especially if additional pre-treatment or separation steps need to be incorporated within the system itself.

#### 3.2 Flow control using valves

For applications involving saliva analysis in  $\mu$ PADs, the use of passive and automated valves has been widely considered to allow multistep assays with more controllable fluid transport. Simple and soluble valves, including those based on sugars such as trehalose, which dissolve in a specific solvent without interfering with subsequent chemical reactions, have been reported in the literature.<sup>104</sup> Materials such as wax and chitosan have also been investigated because their physicochemical properties are sensitive to solvents, temperature or pH.<sup>105–107</sup> Chen *et al.* proposed an innovative approach using wax valves

printed directly on paper, which remain stable until manually opened with the addition of organic solvents such as ethanol, as can be seen in Fig. 4A. Once opened, these valves do not interfere with the subsequent capillary flow, allowing for point-by-point control of reagent release in distance-based detection assays.<sup>106</sup> The device has been used to quantify salt/milk and glucose in human saliva, achieving a limit of detection 11 times lower than previously reported.

Jiang *et al.* developed a simple and portable technique for the fabrication of  $\mu$ PADs with fluid control based on wettability modulation, using a manual corona generator. The strategy involves modifying the paper surface with octadecyltrichlorosilane (OTS) to render it hydrophobic, followed by selective exposure to a corona discharge through a mask to locally restore hydrophobicity in the desired areas.<sup>108</sup> This method allowed the development of an 'on-valve', which is punctually activated by the corona to control the onset of fluid movement in the device. The viability of the system was demonstrated in colorimetric assays for the detection of nitrite in real saliva samples. More advanced technologies have also been proposed, such as electro-osmotic valves combined with hydrophobic barriers, capable of performing protocols such as LAMP directly on raw saliva samples with temperature and

flow control *via* PCBs, as shown in Fig. 4B. A programmable mechanical valve array was also proposed by Rofman *et al.*,<sup>109</sup> which allows parallel and multiplexed control of up to 16 channels in the same device, and was successfully applied to the quantification of glucose in artificial saliva.

## 4. Detection techniques for salivary diagnostics on $\mu$ PADs

In the field of salivary analysis, colorimetric and electrochemical detection methods have been widely explored due to their alignment with the core principles of  $\mu$ PADs, such as low cost, miniaturization, and portability. These techniques allow visual readouts or require only simple instrumentation, making them ideal for point-of-care applications.<sup>16</sup> More recently, the combination of both detection approaches has emerged as a promising strategy to address the individual limitations of each method.<sup>55</sup> This section highlights the key features, applications, and integration strategies of colorimetric, electrochemical, and hybrid detection systems specifically tailored for saliva-based diagnostics.

### 4.1 Colorimetric approaches

Colorimetric detection is one of the most widely used detection techniques in PADs, particularly in clinical diagnostics. This preference is attributed to its operational simplicity, immediate visual feedback, rapid analytical response, portability, low cost, and satisfactory reagent stability.<sup>85,110</sup> The principle of this technique is based on the formation of a colored product resulting from the interaction between the target analyte and reagents previously immobilized in the detection zones of the device.<sup>111</sup>

Colorimetric measurements have been successfully applied to the detection of a broad range of salivary biomarkers. Metabolic markers, such as glucose,<sup>85,111</sup> cholesterol,<sup>85</sup> lactate,<sup>55,85</sup> calcium,<sup>112</sup> and magnesium,<sup>113</sup> have been effectively measured using this technique. Electrolytes and enzymatic biomarkers, including nitrite,<sup>61,114</sup>  $\alpha$ -amylase,<sup>55,91,115</sup> urease,<sup>116</sup> thiocyanide<sup>87</sup> and uric acid,<sup>117</sup> have also been targeted. Furthermore, salivary detection of hormonal and immunological markers, such as cortisol,<sup>118</sup> interleukins,<sup>119</sup> and alpha-fetoprotein,<sup>80</sup> demonstrates the versatility of colorimetric methods. In addition to biomarker detection, colorimetry has been used to identify disease-specific targets, including monkeypox,<sup>115</sup> SARS-CoV-2,<sup>14,120</sup> and Influenza A and B.<sup>121</sup> It has also shown potential in forensic applications, such as the detection of ethanol and phytocannabinoids in saliva.<sup>122</sup>

The reaction mechanisms on which the colorimetric detection is based can be divided into enzymatic and non-enzymatic processes. As depicted in Fig. 5, both enzymatic and non-enzymatic detection strategies have been applied in  $\mu$ PADs for salivary analysis. Enzymatic reactions are especially popular due to their high specificity and their capacity to produce detectable products or by-products that interact with chromogenic indicators.<sup>6,93</sup> A well-known application is the colorimetric

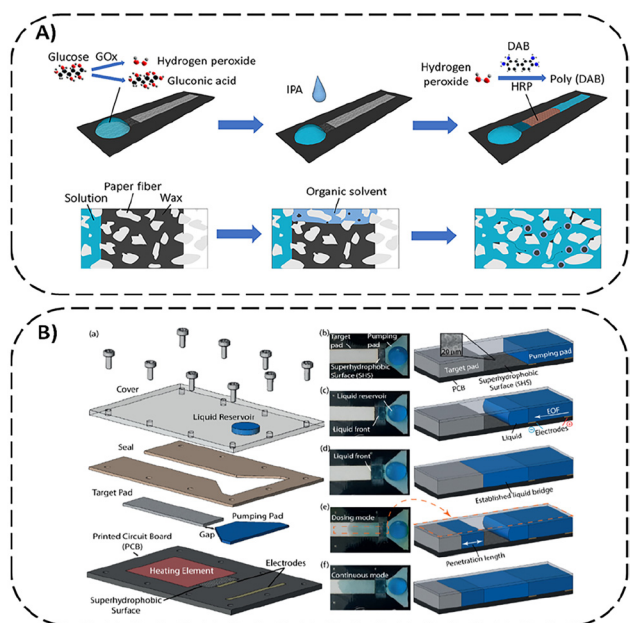


**Fig. 4** (A) Schematic of a  $\mu$ PAD with integrated valves for distance-based glucose detection. (B) Illustration of the electroosmotic pumping valve (EOPV). The exploded view shows the layered assembly: (a) PCB with electrodes and a superhydrophobic surface, porous paper pads connected to the reservoir and detection zone, and a silicone seal forming the hydrophobic gap. Panels (b–f) depict the key operational stages of the valve: (b) valve in the closed state due to Laplace pressure; (c) initial electroosmotic activation; (d) formation of a liquid bridge between the pads; (e) "dosing mode" with intermittent flow; and (f) "continuous mode" enabled by a stable liquid bridge and sustained electroosmotic flow. Reprinted from Chen *et al.*<sup>106</sup> and Rofman *et al.*<sup>109</sup> respectively, with permission.

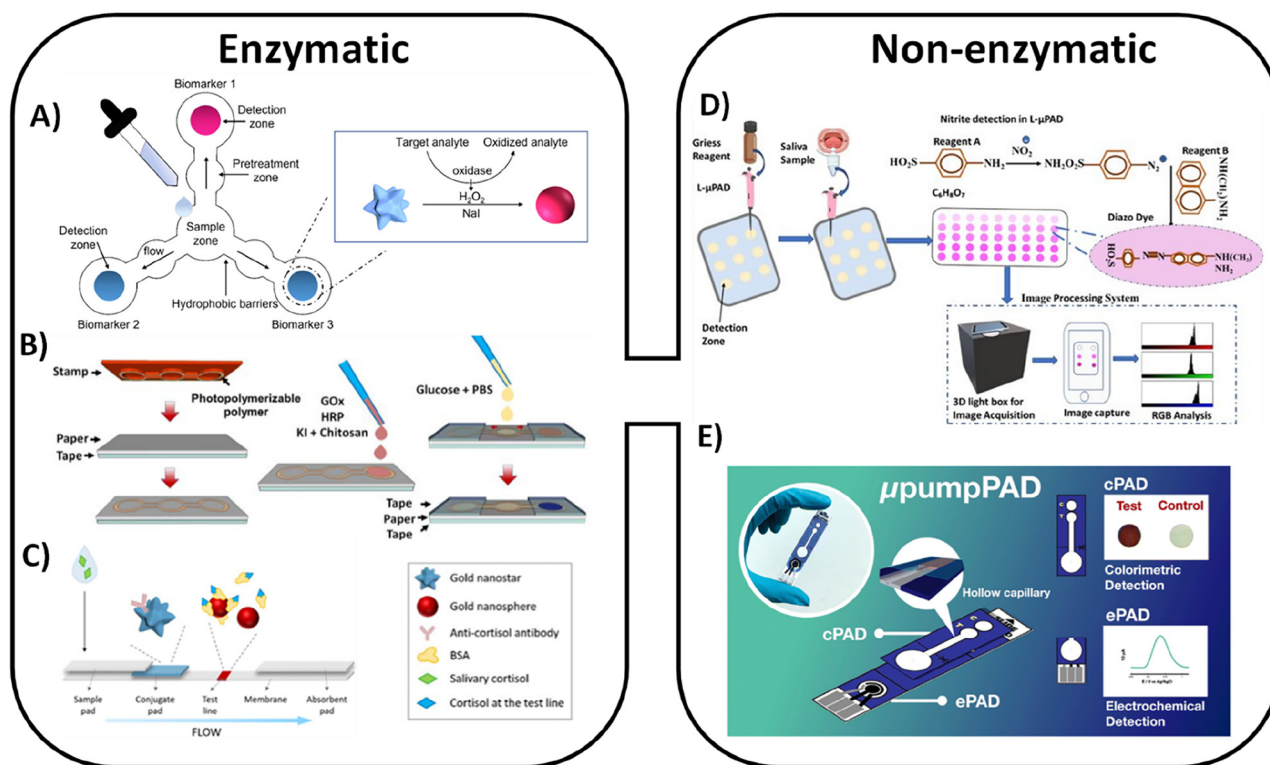


**Fig. 5** Examples from literature illustrating the enzymatic (left column) and non-enzymatic (right column) detection protocols using PADs. Panel (A) presents a general schematic of enzymatic detection mechanisms, with a focus on glucose oxidase (GOx)-based strategies, as exemplified in (B). Panel (C) shows the application of a similar enzymatic principle within a flow-injection analysis (FIA) system for the detection of cortisol. On the non-enzymatic side, a wide range of target analytes can be detected. Panel (D) depicts a representative approach for nitrite detection, one of the most well-established inorganic assays in salivary PADs, while panel (E) illustrates a dual-detection device developed for the analysis of thiocyanate. Reprinted from Scarsi *et al.*,<sup>118</sup> Gölcez *et al.*,<sup>111</sup> Pomili *et al.*,<sup>85</sup> Chanu *et al.*,<sup>114</sup> and Pungjunun *et al.*,<sup>87</sup> respectively, with permission.

detection of glucose using glucose oxidase (Gox), which catalyzes the oxidation of glucose to gluconic acid, producing hydrogen peroxide (H<sub>2</sub>O<sub>2</sub>) as a by-product (see Fig. 5A and B). In the presence of peroxidase, H<sub>2</sub>O<sub>2</sub> reacts with a chromogenic substrate, such as potassium iodide, to form a colored compound that serves as a visible indicator of glucose concentration. The reaction mechanisms underlying colorimetric detection can be broadly categorized into enzymatic and non-enzymatic processes.<sup>111</sup>

Pomili *et al.* demonstrated the use of oxidase enzymes, such as glucose oxidase, lactate oxidase and cholesterol oxidase, which generate hydrogen peroxide (H<sub>2</sub>O<sub>2</sub>) as a by-product, in combination with plasmonic multibranching gold nanoparticles. These nanoparticles exhibited a distinct color shift from blue to pink in response to H<sub>2</sub>O<sub>2</sub>, enabling sensitive colorimetric detection.<sup>85</sup> Interestingly, the same nanoparticles were also used in a non-enzymatic colorimetric assay for the detection of cortisol, highlighting their versatility, as illustrated in Fig. 5C.<sup>118</sup> Another strategy is the targeting of enzymes naturally present in saliva. Silva-Neto *et al.* reported a protocol to quantify α-amylase activity by monitoring the formation of a dark starch-iodine complex catalyzed by the enzyme.<sup>91</sup> Similarly, Ferreira *et al.* measured urease activity by the color change of bromothymol blue triggered by the release

of ammonia during urea hydrolysis by endogenous urease.<sup>116</sup> These approaches need to account for variability in enzyme concentration in different saliva conditions, which can affect signal intensity and lead to inconsistent interpretation of results in point-of-care diagnostics. A classic example is the colorimetric detection of glucose using glucose oxidase, which can produce different results in fasting or postprandial states.

Non-enzymatic reactions, while generally less specific for certain clinical screenings, remain highly relevant in colorimetric salivary analysis due to their simplicity and broad applicability. Unlike enzymatic methods, which often rely on specific biological interactions, non-enzymatic detection can target analytes that occur naturally in saliva, are introduced through toxic exposure, or result from metabolic processes intrinsic to the host or associated pathogens. A representative example is ethanol detection, as reported by Srisomwat *et al.*, where acidified potassium dichromate acts as an oxidizing agent, converting ethanol into acetic acid while being reduced to chromium(III) ions (Cr<sup>3+</sup>), which produce a characteristic greenish-brown color.<sup>123</sup>

Among non-enzymatic mechanisms, complexation reactions stand out for their operational simplicity and ability to form stable, colored products. Notable examples include the Griess reaction for nitrite detection (see Fig. 5D),<sup>110,114</sup>

calcium complexation with methylthymol blue (MTB)<sup>124</sup> or cresolphthalein,<sup>112</sup> the reaction between eriochrome cyanine and magnesium,<sup>113</sup> and the use of Fast Blue B Salt (FBBS) for detecting THC.<sup>123</sup> Despite their advantages, the lower specificity of non-enzymatic approaches can pose challenges in clinical contexts, particularly when selectivity is essential for accurate diagnosis. Other relevant ions in saliva, such as thiocyanate and iron, have also been successfully detected through complexation reactions. Thiocyanate reacts with ferric ions ( $\text{Fe}^{3+}$ ) to form the reddish-brown  $[\text{FeSCN}]^{2+}$  complex, a widely used reaction for colorimetric detection in saliva, as represented in Fig. 5E,<sup>87</sup> while iron itself can be quantified using chromogenic ligands, such as 1,10-phenanthroline, which forms an orange-red complex with  $\text{Fe}^{2+}$ .

Colorimetric detection offers multiple strategies for signal readout, each with distinct advantages and limitations depending on the context of the application. The most basic method is visual inspection, a long-standing technique that requires no instrumentation, making it ideal for low-cost, rapid, and user-friendly testing—especially in POC scenarios.<sup>125</sup> This approach is particularly suited for qualitative or semi-quantitative assessments, including binary (positive/negative) tests, such as those used for SARS-CoV-2 spike protein detection.<sup>126</sup> Visual readouts are also commonly employed in lateral flow assays, where the presence of a target analyte is indicated by a colored line in the test zone,<sup>121</sup> as demonstrated in multiplexed tests for SARS-CoV-2 and influenza viruses.<sup>121</sup>

To enhance the precision and reproducibility of color interpretation, visual detection has often been complemented or replaced with digital image colorimetry (DIC). DIC involves capturing images of the detection zone using devices such as smartphones, scanners, or webcams, followed by quantitative analysis of color intensity using image-processing software.<sup>127</sup> While this method increases analytical accuracy, it requires consistent lighting conditions and image standardization—factors that, if not carefully controlled, can affect reliability. Flatbed scanners offer excellent light stability but reduce portability, while smartphones provide greater flexibility but often require custom holders or light-controlled boxes to ensure reproducibility.<sup>85,117</sup>

An emerging alternative is distance-based detection (DBD), which merges visual simplicity with quantification. In this technique, the analyte flows through a microchannel containing colorimetric reagents, forming a colored band whose length correlates with analyte concentration.<sup>128,129</sup> DBD enables straightforward quantification without instrumentation, but its use in salivary diagnostics remains limited. Notable applications include interleukin detection using straight channels<sup>119</sup> and iodide analysis in semicircular channels based on angular distance.<sup>130</sup>

While colorimetric methods remain attractive for their simplicity, their sensitivity and quantification range can be limited compared to more advanced techniques. These constraints have encouraged the integration or substitution of colorimetry with more sensitive platforms, such as electro-

chemical detection, especially in applications requiring precise biomarker quantification.

Furthermore, the integration of machine learning (ML) algorithms has emerged as a transformative strategy in colorimetric  $\mu$ PADs, particularly in smartphone-based analytical platforms. Beyond compensating for variations in ambient lighting and camera heterogeneity, ML enables multidimensional pattern recognition from RGB and texture features, improving signal discrimination and analytical robustness. Convolutional neural networks (CNNs), Random Forest, and ensemble learning models have demonstrated enhanced performance in paper-based colorimetric systems, including  $\mu$ PADs for lactate and glucose detection.<sup>131–133</sup>

In saliva-based applications, where matrix complexity, turbidity, and viscosity introduce non-linear signal distortions, regression-based ML approaches outperform traditional linear calibration by modeling complex data relationships.

## 4.2 Electrochemical approaches

Electrochemical detection relies on measuring electrical signals generated by redox reactions occurring at the interface between the analyte and an electrode, enabling the quantification of specific biomarkers in saliva.<sup>134</sup> This technique encompasses various methods, including voltammetry, amperometry, potentiometry, and electrochemical impedance spectroscopy (EIS) analyses, each offering distinct advantages based on the analyte's properties and the salivary matrix characteristics.<sup>135</sup> Among these, voltammetry is the most widely used method in salivary analysis due to its ability to provide high sensitivity and precise measurements. Cyclic voltammetry, for instance, is often employed to detect electroactive compounds,<sup>136</sup> while square-wave voltammetry has found use in detecting phenylamine.<sup>137</sup> However, differential pulse voltammetry stands out as the most commonly applied technique, being particularly useful for detecting biomarkers such as histamine,<sup>138</sup> homocysteine, C-reactive protein,<sup>139</sup> and the SARS-CoV-2 spike protein.<sup>69</sup>

While voltammetry remains dominant, other electrochemical techniques have also been explored in saliva diagnostics, albeit less frequently. Amperometry offers rapid detection and is often used for glucose monitoring,<sup>140</sup> whereas potentiometry has proven effective in ion-selective assays, such as for naproxen.<sup>140</sup> Additionally, EIS provides label-free detection and has been applied for the identification of pathogens such as the monkeypox virus.<sup>141</sup>

One critical challenge of electrochemical methods, however, is that they require the analyte to be electroactive. This limitation has driven the development of strategies to either enhance the electrochemical response of non-electroactive analytes or enable the detection of their by-products. One approach is chemical derivatization, where target molecules, such as phenylamine, are converted into electroactive compounds *in situ*. Another strategy involves electrode surface modification, which can involve the immobilization of specific reagents or nanomaterials to increase sensitivity and speci-

ficity. For example, Diao *et al.* developed an ion-selective electrode or the functionalization of electrodes with eutectic Ga–In and Au nanoparticles to capture aptamers specific to biomarkers such as homocysteine and C-reactive protein.<sup>139</sup>

In addition, aptamer-based sensors have gained traction, offering high selectivity through molecular recognition, as seen in histamine detection.<sup>138</sup> Another promising method is the use of enzymatic cascades to amplify electrochemical signals, where enzymes, such as oxidases, produce electroactive species like hydrogen peroxide (H<sub>2</sub>O<sub>2</sub>), which can then interact with the electrode. This approach has been successfully applied for glucose and uric acid detection,<sup>15</sup> with further amplification achieved by combining glucose oxidase with redox compounds such as aminoferrocene.<sup>140</sup>

Although electrochemical detection offers improved sensitivity, electrode fouling due to salivary proteins and mucins remains a persistent challenge. Additionally, the requirement for external readers or potentiostats may limit full decentralization unless fully integrated low-cost electronics are implemented. However, electrochemical methods are not limited to standalone techniques. Many studies have explored hybrid systems, where electrochemical detection is integrated with other methods such as colorimetry. These combined approaches offer the potential to overcome the individual limitations of each method, improving the robustness and sensitivity of paper-based analytical platforms for salivary diagnostics.

### 4.3 Integration of detection techniques

The integration of different detection methods within  $\mu$ PADs has emerged as a powerful strategy to enhance sensitivity, specificity, and overall analytical robustness. By leveraging the complementary strengths of each technique—such as the visual simplicity of colorimetry and the quantitative precision of electrochemical detection—these hybrid systems contribute to the development of more efficient, reliable, and user-friendly diagnostic platforms. This is particularly beneficial for POCT and self-monitoring scenarios, where ease of use and rapid results are critical.

Fabiani *et al.* demonstrated this synergy in a paper-based electrochemical immunosensor for COVID-19, combining a colorimetric readout using 3,3',5,5'-tetramethylbenzidine (TMB) with amperometric detection.<sup>142</sup> The initial color change acted as a visual indicator, signaling the correct reagent flow and guiding users to initiate electrochemical measurements *via* a smartphone interface. This dual approach minimized user error while preserving assay reliability. The schematic shown in Fig. 6A highlights the device function.

Similarly, Pungjunun *et al.* integrated colorimetric and electrochemical techniques for the detection of salivary thiocyanate. The reddish-brown [FeSCN]<sup>2+</sup> complex formed during the colorimetric reaction was quantified using smartphone-assisted DIC, and the same sample was subsequently analyzed by square-wave voltammetry. This sequential dual analysis

achieved a lower detection limit than colorimetric detection alone, demonstrating that integration can improve analytical sensitivity.<sup>87</sup>

In addition to performance gains, hybridization of detection methods also enables multiplexed analysis. Fotouhi *et al.* reported a PAD capable of simultaneously detecting dopamine and iodide *via* linear sweep voltammetry and DBD measurements, respectively.<sup>130</sup> A colorimetric reaction involving the formation of a blue iodine-starch complex was enhanced by applying a low-voltage potential, bridging the colorimetric and electrochemical modalities within a single system.

Further expanding this concept, Sousa *et al.* developed a  $\mu$ PAD capable of detecting multiple salivary analytes—including lactate, nitrite, pH, and  $\alpha$ -amylase—using a shared sampling zone and integrated electrodes. Electrochemical detection of lactate was achieved through chronoamperometry using electrodes modified with Prussian blue nanocubes, while nitrite, pH, and amylase were measured through smartphone-assisted DIC using tailored colorimetric reactions.<sup>55</sup>

In another example, Lima *et al.* combined both detection modes on commercial wooden tongue depressors to achieve simultaneous measurement of glucose, uric acid, thiocyanate, and nitrite, without sample preprocessing, as can be seen in Fig. 6B. While nitrite and thiocyanate were detected through colorimetric measurements, glucose and uric acid required chronoamperometric detection using custom-designed electrodes.<sup>143</sup>

### 4.4 Other detection techniques

In addition to colorimetric and electrochemical approaches, other detection methods have been explored in conjunction with  $\mu$ PADs for saliva analysis. One such method is fluorescence, which uses fluorescent probes to detect specific targets in saliva, offering high sensitivity and the ability to perform real-time measurements. Techniques such as fluorescence resonance energy transfer (FRET) have been used to detect biomarkers in saliva with high precision.<sup>10</sup>

Another emerging technology is electrochemical impedance biosensors,<sup>22</sup> an approach derived from electrochemical methods, which measure changes in the electrical resistance of an electrode–sample interface due to interaction with the analyte. This method is particularly useful for detecting proteins and cells in saliva and offers a promising alternative for rapid and sensitive testing. In addition, impedance spectroscopy and Raman spectroscopy have been used in  $\mu$ PADs for the non-invasive detection of biomarkers in saliva, allowing the detection of compounds with high selectivity without the need for chemical reagents. These techniques complement traditional methods and provide a wider range of options for detecting a variety of analytes in saliva samples, with the potential to expand the applicability of  $\mu$ PADs in clinical and POC diagnostics.

The choice of detection technique depends on several factors, but the most critical aspect to consider is the chemical nature of the target analyte. Following this, other criteria such

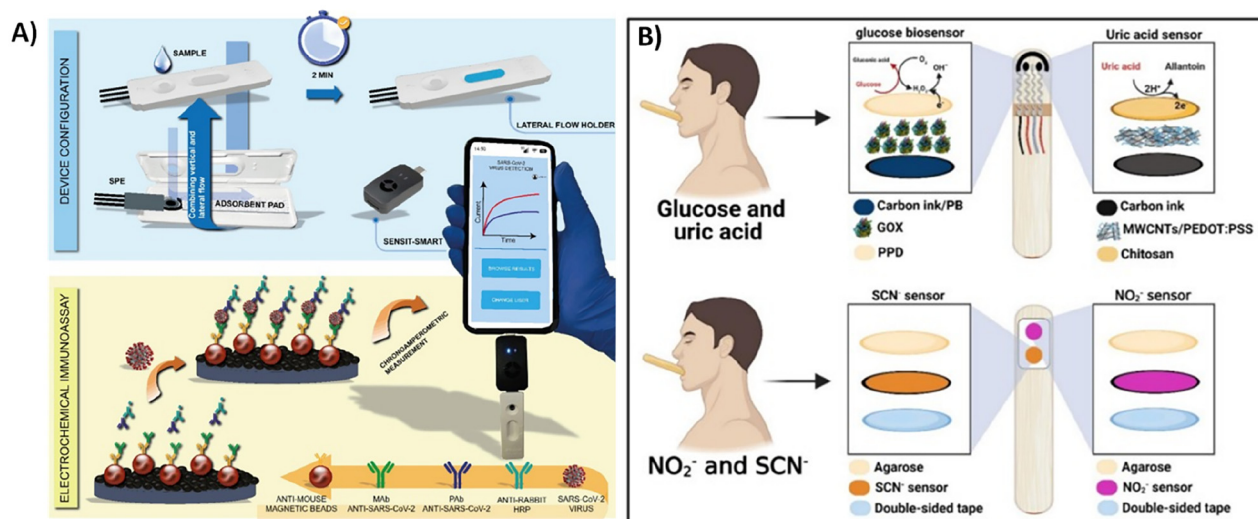


**Fig. 6** Examples of integrated detection strategies in PADs for salivary analysis. (A) Schematic of a dual-mode PAD developed by Fabiani *et al.*, where a colorimetric reaction with TMB guides the user for subsequent amperometric detection via a smartphone interface. (B) Application of a wooden tongue depressor-based PAD combining colorimetric (for nitrite and thiocyanate) and electrochemical (for glucose and uric acid) detection, enabling the simultaneous analysis of multiple salivary biomarkers without sample preprocessing. Reprinted from Fabiani *et al.*,<sup>142</sup> and de Lima *et al.*,<sup>141</sup> respectively, with permission.

as cost, equipment requirements, and methodological limitations should also be evaluated. Table 1 presents a comparative overview of common detection techniques, highlighting

key parameters typically considered when selecting an appropriate analytical protocol for salivary biomarker detection using  $\mu$ PADs.

**Table 1** Comparative summary of the detection methods in PADs for salivary analysis

	Colorimetric	Electrochemical	Integrated systems (colorimetric + electrochemical)	Other approaches (fluorescence, microscopy, and Raman)	Ref.
Detection principle	Color change in response to analyte interaction	Measurement of electrical signals (current, potential, or impedance)	Combination of colorimetric signal and electrical signal for cross-validation or enhanced sensitivity	Detection of fluorescence emission, impedance changes, or Raman scattering	127, 146 and 147
Required equipment	None (naked eye or DBD <sup>a</sup> ); smartphone, scanner, camera, and computer for DIC <sup>b</sup>	Potentiostat (benchtop or portable), smartphone or computer, and electrodes	Equipment for both techniques (potentiostat + camera/smartphone)	Depends on technique (fluorescence reader, microscope, or spectrometer)	44, 47, 86, 148 and 149
Sensitivity and specificity	Moderate sensitivity (often enhanced with DIC <sup>b</sup> ); good specificity with enzymatic reactions; and lower in non-enzymatic methods	High sensitivity, especially with modified electrodes and high specificity with aptamers, enzymes, or selective electrodes	Enhanced robustness, sensitivity, and specificity through cross-validation	High sensitivity and specificity; depends on the technique employed	150–152
Cost and simplicity	Very low cost; highly simple	Moderate cost (requires electrodes and reader); greater complexity	Variable cost and complexity; generally moderate to high	High cost and complexity; requires specialized equipment and training	67 and 68
Sample preparation needs	Generally minimal; depends on saliva viscosity and may be integrated into the system	May require filtration, dilution, or derivatization	Compatible with minimal pre-treatment; same sample used in both readings	May require specific preparation or labeling of the analyte	31, 153 and 154
Limitations	Lower sensitivity in quantitative analyses; matrix interference	Requires electroactive analytes, modified electrodes, or derivatization; higher cost	Greater operational and fabrication complexity	High cost; need for specialized equipment and limited portability	103, 129, 155 and 156

<sup>a</sup> DBD = distance-based detection. <sup>b</sup> DIC = digital image colorimetry.

## 5. Salivary biomarkers and applications in clinical diagnostics

Saliva-based diagnostics using  $\mu$ PAD have attracted considerable research attention due to several distinct advantages over other biological fluids, such as blood.<sup>143,144</sup>

Saliva collection is non-invasive, painless, and can be performed easily without specialized personnel or equipment, reducing both costs and patient discomfort. Unlike blood, saliva does not undergo fibrin-mediated coagulation, which simplifies sample handling and eliminates the need for anticoagulants during processing. In addition, saliva is comparatively easy to manipulate, and, depending on the target biomarker and storage conditions, may remain analytically stable for up to 24 h at room temperature and for several days under refrigeration, depending on the biomarker of interest. These properties make it an attractive biological fluid for biochemical and toxicological assessments.<sup>7</sup> Saliva plays multiple physiological roles, including lubrication, antimicrobial protection, food-bolus formation, swallowing, and facilitating speech. Salivary secretion is primarily carried out by three major glands: the parotid, saliva submandibular, and sublingual glands. These glands are composed of serous and mucous cells—serous cells produce a watery secretion, while mucous cells contribute a thicker, more viscous component.<sup>4,157</sup>

On average, a healthy adult produces approximately 600 mL of saliva per day. Its composition is predominantly water (about 99%) mixed with electrolytes such as sodium, potassium, and chloride. In addition, saliva contains proteins, such as amylases, that aid digestion and antimicrobial agents that help regulate the oral microbiota. Other constituents include metabolic byproducts (urea, ammonia), blood-derived components, gingival crevicular fluid, and microbial components, including bacteria and their metabolites.<sup>5,6</sup>

As shown in Table 2, saliva is particularly advantageous due to its ease of collection and the relatively small volume required (1–4 mL). This makes it highly suitable for rapid and on-site diagnostics. In contrast, blood collection requires a more invasive procedure, while urine and sweat, although non-invasive, require larger volumes and can be affected by more

significant interferences such as pH or salts. However, the concentration of biomarkers in saliva tends to be lower than in blood and urine. Nevertheless, its suitability for paper-based devices remains high, with minimal need for complex extraction or separation modules. Despite common interferences from enzymes, mucins, and food particles, saliva remains a promising diagnostic tool, particularly when combined with advances in sensor technology to detect specific biomarkers.

### 5.1 Salivary collection and processing

The main advantage of using saliva for diagnostic testing lies in its ease and flexibility of collection, which can be performed using simple tools such as plastic tubes, absorbent swabs, or commercially available collection devices. This practical approach is especially relevant for POC applications, which are designed to deliver rapid, decentralized diagnostic results without the need for laboratory infrastructure or trained professionals. The feasibility of collecting saliva in non-clinical settings expands the reach of PADs, making them ideal for use in remote areas or for self-monitoring.

Saliva can be collected through two main approaches: unstimulated (or resting) saliva and stimulated saliva. Unstimulated saliva is predominantly secreted by the submandibular and sublingual glands in the absence of external stimuli.<sup>30</sup> It reflects the basal state of salivary secretion and contains essential components, such as electrolytes, mucins, and antimicrobial proteins, which are crucial for maintaining mucosal integrity, lubrication, and innate defence mechanisms.<sup>11</sup>

In contrast, stimulated saliva is produced in response to gustatory, olfactory, or mechanical stimuli, such as chewing or tasting acidic substances. This type of saliva is primarily secreted by the parotid glands, accounting for approximately 80% of the total stimulated flow. It is typically waterier and contains higher bicarbonate concentrations, which contribute to its buffering capacity and help neutralize acids in the oral cavity.<sup>5</sup>

Following collection, saliva samples often require pre-treatment to ensure stability and analytical accuracy. Common processing techniques include centrifugation, filtration, and cryopreservation, as well as the addition of chemical preservatives

**Table 2** Comparative analysis of the biological fluids and their suitability for paper-based analytical devices

Characteristic	Saliva	Urine	Blood	Sweat	Ref.
Easy-to-collect	Very easy (not stimulated)/easy (stimulated)	Easy	Requires puncture	Easy	11
Invasiveness	Non-invasive	Moderately invasive	Highly invasive	Non-invasive	12 and 158
Collection volume	Moderate, usually 1–4 mL	Abundant	Moderate, ~1 mL	Low	62, 159 and 160
Suitability for paper-based devices	Highly suitable	Highly suitable	Suitable (usually requires incorporating an extraction/separation module into the device)	Suitable	161–163
Common interferences	Enzymes, mucins, and food	Salts and pH	Hemoglobin and lipoproteins	Salts and pH	145, 164 and 165
Concentration of biomarkers	Medium	High	High	Low	30, 109 and 166

to prevent enzymatic degradation and microbial contamination.<sup>11</sup> In several  $\mu$ PAD applications, saliva samples are used without any extensive pretreatment. This is largely due to the fact that the porous structure of paper, when integrated with microfluidic channels, can naturally retain certain interferences and particulate matter, thus simplifying sample processing. However, it is important to note that, depending on the nature of the target analyte, particularly in the case of low abundance biomarkers or analytes susceptible to degradation, pre-analytical steps such as filtration, stabilisation, or selective enrichment may still be required to ensure analytical reliability and sensitivity.

This approach is supported by recent studies demonstrating that the intrinsic porosity and capillarity of paper used in  $\mu$ PADs can selectively retain particulate matter and potential interferents during fluid migration, enabling the direct use of untreated saliva samples in many point-of-care applications. Ferreira *et al.* successfully quantified nitrate and nitrite in human saliva using a paper-based device without prior sample processing, while Chen *et al.* highlighted that, although paper microfluidics can simplify or even eliminate pre-treatment steps, the necessity for such steps should still be evaluated based on the physicochemical characteristics and stability of the target analyte.<sup>167,168</sup>

In conventional laboratory diagnostics, saliva samples are frequently centrifuged to remove cellular debris, followed by storage at  $-20\text{ }^{\circ}\text{C}$  or  $-80\text{ }^{\circ}\text{C}$  prior to analysis by ELISA, HPLC, LC-MS/MS, or RT-PCR, depending on the analyte. Therefore, when  $\mu$ PADs are proposed as alternatives, their analytical performance should ideally be compared with these reference protocols using matched clinical samples.<sup>2,48</sup>

## 5.2 Salivary biomarkers

Disease diagnosis using  $\mu$ PADs and saliva as a biofluid is a promising approach due to the wide range of analytes naturally present in saliva, including ions, antibodies, microbial metabolites, hormones, enzymes, and even whole microorganisms.<sup>145</sup> The concentration and composition of these salivary components are correlated with numerous oral and systemic conditions, including infectious, inflammatory, metabolic and neoplastic diseases. In addition, such approaches fit well with the ASSURED criteria, a set of characteristics defined by the World Health Organization (WHO) for ideal point-of-care diagnostics.<sup>169,170</sup>

Salivary analytes can be classified in several categories, including their chemical nature, diagnostic relevance, and functional role in disease detection. Table 3 provides a classification based on the chemical characteristics and diagnostic purpose of these biomarkers, along with recent examples from the literature illustrating their application in paper-based devices. Categorizing biomarkers according to their chemical nature allows for a more structured and focused review of what has been reported, especially considering that a given disease, whether systemic or localized, may involve multiple biomarkers, which together contribute to a more accurate and comprehensive diagnosis.

**5.2.1 Acid and inorganic compounds.** This category includes small molecules and ions naturally present in saliva that can indicate both oral and systemic health conditions. Examples include salivary pH,<sup>55</sup> nitrite,<sup>16,61,171</sup> nitrate,<sup>167,172</sup> ammonia,<sup>12</sup> phosphate,<sup>173,174</sup> uric acid,<sup>176,177</sup> and metallic ions, such as magnesium ( $\text{Mg}^{2+}$ ),<sup>113</sup> calcium ( $\text{Ca}^{2+}$ ),<sup>124</sup> and iron ( $\text{Fe}^{2+}$ ).<sup>158</sup>

Paper-based devices have been successfully developed to measure many of these analytes. For example,  $\mu$ PADs functioning as pH indicators enable the monitoring of salivary pH variations, which are often linked to caries risk and periodontal diseases. Nitrite and nitrate levels can reflect bacterial activity or inflammatory states, whereas ions such as calcium and phosphate are directly associated with tooth demineralization or salivary gland function.<sup>167,173</sup> However, despite their analytical accessibility, matrix effects, such as variable ionic strength, enzymatic degradation or protein adsorption, can affect both the stability and reactivity of colorimetric reagents.

Clinically, these analytes are commonly quantified using ion chromatography, spectrophotometry, enzymatic assays, or automated biochemical analysers. For example, salivary uric acid and ammonia are often measured using enzymatic-colorimetric kits adapted from serum analysis, while nitrite and nitrate are quantified *via* Griess-based spectrophotometric assays or chromatographic techniques.<sup>7,16,48,129</sup>

In the context of systemic disease,  $\mu$ PADs targeting these analytes have emerged as promising for the early detection of metabolic disorders and even certain cancers. For instance, uric acid and ammonia levels have been explored as markers for metabolic dysfunctions and kidney disease,<sup>194</sup> while broader applications include detection strategies for lung, oral, and breast cancer using salivary profiles.<sup>195–197</sup>

Strategies such as buffer pre-loading or the use of hydrophilic membranes can help minimize matrix-related interferences, including variations in pH, viscosity, and biofouling effects. For example, Aguiar *et al.* demonstrated improved analytical performance using modified cellulose papers that enhance sample transport and reduce matrix interferences.<sup>112</sup>

Multiplexed platforms for the simultaneous detection of ions, such as phosphate and nitrate, have clinical appeal for distinguishing systemic causes from localized oral conditions.<sup>174</sup> However, ensuring that cross-reactivity is avoided in confined test zones remains a technical obstacle. The use of separation microfluidic channels offers a way to improve selectivity in such applications.<sup>124</sup>

**5.2.2 Proteins and enzymes.** Proteins and enzymes represent a more complex class of salivary biomarkers, requiring higher sensitivity and specificity. In routine clinical laboratories, salivary proteins and enzymes are typically quantified using ELISA or automated immunoassay platforms, which provide high sensitivity and standardized calibration. Comparisons between  $\mu$ PAD-based assays and ELISA have, in some cases, shown strong linear correlations, particularly for  $\alpha$ -amylase and CRP.<sup>2,198,199</sup> In recent advances, Silva-Neto *et al.* demonstrated the successful integration of salivary amylase assays into paper-based formats using enzyme-substrate color

**Table 3** Classification of the potential salivary biomarkers by their chemical nature and diagnostic role

Biomarker	Clinical relevance	Normal range in saliva	Main associated techniques	LOD	Ref.
Salivary pH	Reflect nitric oxide pathway activity and indicators of inflammation, infection, cardiovascular and periodontal diseases.	6.5–7.5	Colorimetric indicators	—	55
Nitrite	Reflect nitric oxide pathway activity and indicators of inflammation, infection, cardiovascular and periodontal diseases.	25–1000 $\mu\text{mol L}^{-1}$	Colorimetric detection (Griess method)/ electrochemical	0.05 $\mu\text{mol L}^{-1}$ / 1.5 $\mu\text{mol L}^{-1}$	167 and 171
Nitrate		5–300 $\mu\text{mol L}^{-1}$	Colorimetric and electrochemical detection	0.08 $\text{mmol L}^{-1}$ / 0.015 $\mu\text{mol L}^{-1}$	167 and 172
Magnesium ( $\text{Mg}^{2+}$ ) Iron ( $\text{Fe}^{2+}$ ) Calcium ( $\text{Ca}^{2+}$ ) Phosphate	Involved in bone health, cardiovascular function, energy metabolism, and immune response.	0.1–0.5 $\text{mmol L}^{-1}$ 10–30 $\mu\text{g dL}^{-1}$ 1.1–2.5 $\text{mmol L}^{-1}$ 4–8 $\text{mmol L}^{-1}$	Colorimetric detection Colorimetric detection Colorimetric detection Colorimetric and electrochemical detection	62 $\mu\text{mol L}^{-1}$ 5.6 ppm 2.9 $\text{mg L}^{-1}$ 26 $\mu\text{mol L}^{-1}$ / 26.27 $\text{mg L}^{-1}$	113 158 124 173 and 174
Thiocyanate	Marker of oxidative stress and tobacco use; elevated in periodontal disease.	0.2–2.0 $\mu\text{mol L}^{-1}$	Colorimetric assays and electrochemical sensors	6 $\mu\text{mol L}^{-1}$	87
Ammonia	Reflect liver and kidney function; useful in monitoring CKD <sup>a</sup> and microbiome balance.	2–5 $\text{mmol L}^{-1}$	Colorimetric detection <i>via</i> gas-diffusion $\mu\text{PADs}$	0.03 $\text{mg dL}^{-1}$	12
Urea		15–22 $\text{mg dL}^{-1}$	Colorimetric detection <i>via</i> urease activity	10.4 $\text{mg dL}^{-1}$	175
Uric acid	Correlates with serum levels; useful for monitoring metabolic and cardiovascular conditions.	30–240 $\mu\text{mol L}^{-1}$	Colorimetric assays and electrochemical detection with PEDOT-GO <sup>b</sup> nanocomposites	0.75 $\mu\text{mol L}^{-1}$	176 and 177
Salivary amylase	Digestive enzyme; elevated in stress and pancreatic disorders.	20–100 $\text{U mL}^{-1}$	Colorimetric enzyme activity detection	0.75 $\text{U mL}^{-1}$	91
Lactoferrin	Periodontitis, Alzheimer's disease, and systemic inflammation	2–5 $\text{mg L}^{-1}$	Colorimetric detection	110 $\mu\text{g mL}^{-1}$	178
Alkaline phosphatase (ALP)	Bone diseases, liver diseases, and periodontal disease	20–140 $\text{U L}^{-1}$	Colorimetric enzyme activity detection	1.69 $\text{U L}^{-1}$	179
C-reactive protein (CRP)	Cardiovascular diseases, periodontal disease, and diabetes	0–5 $\text{mg L}^{-1}$	LFA	55 $\text{ng mL}^{-1}$	180
Interleukin-6	Inflammatory and cancer-related biomarkers; involved in tissue degradation and immune response.	1–50 $\text{pg mL}^{-1}$	Colorimetric detection	9.55 $\text{pg mL}^{-1}$	181
Tumor necrosis factor alpha (TNF- $\alpha$ )		2–10 $\text{pg mL}^{-1}$	Electrochemical detection	5.97 $\text{pg mL}^{-1}$	181
Matrix metalloproteinases (MMPs)		Variable ( $\text{ng mL}^{-1}$ )	LFA and electrochemical detection	1.0 $\text{ng mL}^{-1}$	182 and 183
Cortisol	Stress, metabolic, and cardiovascular markers; useful in tracking systemic health.	0–30 $\text{ng mL}^{-1}$	Electrochemical detection	0.81 $\text{ng mL}^{-1}$	184
Cholesterol		0.5–12 $\text{mg dL}^{-1}$	Colorimetric and impedimetric detection	<5 $\mu\text{g mL}^{-1}$	185 and 186
Glucose	Diabetes and metabolic syndrome and dysfunction	0.5–1.0 $\mu\text{mol L}^{-1}$	Colorimetric and electrochemical enzyme activity detection	2.60 $\times 10^{-6}$ $\text{mol L}^{-1}$	88, 187 and 188
Lactate	Sepsis, hypoxia, physical exertion, metabolic disorders, and bacterial activity	0.11–0.56 $\text{mmol L}^{-1}$	Electrochemical detection	8.14 $\times 10^{-7}$ $\text{mol L}^{-1}$	188
Tuberculosis (TB)	Saliva enables rapid, non-invasive detection of infectious agents.	Negative/positive	Nucleic acid amplification and colorimetric detection	1.95 $\times 10^{-2}$ $\text{ng mL}^{-1}$	73
SARS-CoV-2		Negative/positive	Nucleic acid amplification and LFA	30 $\text{ng mL}^{-1}$	142 and 189
Influenza virus		Negative/positive	LFA, colorimetric and electrochemical detection	<5 PFU $\text{mL}^{-1}$	190
Aldehydes	Markers of oxidative stress, oral cancer risk, and substance use.	Not well established; detection range: 20.4–114.0 $\mu\text{M}$	Colorimetric detection	6.1 $\mu\text{mol L}^{-1}$	191
Alcohol (ethanol)		0–0.05 $\text{g dL}^{-1}$	Colorimetric detection	Not specified	146
Codeine and fentanyl	Useful for on-site detection of opioid or stimulant use and monitoring abstinence.	Not established; detectable levels vary with use	LFA and electrochemical detection	Codeine 70 $\text{ng mL}^{-1}$ and fentanyl 22 $\text{ng mL}^{-1}$	192
Methamphetamine		Negative/positive	Electrochemical detection	<400 $\text{ng mL}^{-1}$	193

<sup>a</sup> CKD = chronic kidney disease. <sup>b</sup> PEDOT-GO = poly(3,4-ethylene dioxythiophene).

reactions.<sup>91</sup> While these platforms have improved sensitivity for this group of analytes, challenges remain in ensuring selective detection in the presence of complex salivary matrices.<sup>119,184</sup>

An important gap in this area is the lack of standardized antibody reagents and matrix-stabilization techniques, which hinders reproducibility and shelf-life. The potential for multiplexed protein detection is promising but still in the early stages of development, often constrained by cross-reactivity and signal overlap.<sup>180</sup>

A key challenge is the complex salivary matrix, which can lead to nonspecific binding and protein degradation, especially under uncontrolled conditions. PADs using wax-printed barriers or plasma separation membranes can selectively retain proteins while allowing removal of interfering species, improving both specificity and reliability.<sup>119</sup>

### 5.2.3 Cytokines and an inflammatory biomarker.

Inflammatory biomarkers such as TNF- $\alpha$ , MPO, and MMPs are valuable for monitoring chronic inflammatory diseases, including periodontitis and autoimmune disorders. Despite their diagnostic relevance, few studies have addressed the ultra-low concentrations and instability of these biomarkers in saliva. Clinically, cytokines such as TNF- $\alpha$ , IL-6, and MMPs are predominantly quantified using high-sensitivity ELISA or multiplex bead-based immunoassays.<sup>181–183</sup>

Several devices are currently under development to detect cytokines in saliva, often using electrochemical immunosensors. While references for specific cytokines, such as MPO or TNF- $\alpha$ , were not listed above, many of the platforms from protein and enzyme detection studies can be adapted to target inflammatory mediators with similar approaches.<sup>180,181</sup>

Clinically, the early detection of elevated cytokine levels could significantly impact the monitoring of chronic diseases, such as periodontitis or Sjögren's syndrome. However, this demands  $\mu$ PADs with active pre-concentration steps, such as those employing capillary-based enrichment zones or nanoparticle-assisted signal amplification. These strategies remain underexplored in salivary diagnostics.<sup>200–202</sup>

**5.2.4 Hormones and metabolites.** Hormonal and metabolic markers are important because of their direct association with systemic conditions, such as stress, diabetes, and cardiovascular disease. In clinical practice, salivary cortisol is routinely measured using ELISA or chemiluminescent immunoassays, whereas glucose and cholesterol are quantified through enzymatic-colorimetric assays or automated analyzers.<sup>40,48,129</sup>

Devices developed by different authors have shown promising results in noninvasive glucose and cortisol monitoring. However, devices often struggle with dynamic range and time-dependent variability in salivary hormone levels, which may limit their standalone diagnostic potential.<sup>55,86,185</sup>

The integration of electrochemical sensing platforms represents a step toward quantitative  $\mu$ PADs, though such systems must address challenges related to calibration, stability, and signal drift. Future clinical applications would benefit from continuous monitoring formats or wearable integration, particularly in stress research or diabetes management, where

real-time salivary readings could complement CGMs (continuous glucose monitors).<sup>187,189</sup>

**5.2.5 Pathogens.** Pathogen detection is one of the most impactful areas of research involving paper microfluidics, especially for diseases with high transmission rates. The COVID-19 pandemic highlighted the crucial role of rapid, saliva-based diagnostics. The clinical gold standards for pathogen detection in saliva typically include RT-PCR for viral RNA, culture-based methods for bacteria, or antigen-based immunoassays. During the COVID-19 pandemic, several  $\mu$ PAD platforms were benchmarked against RT-PCR and reported high sensitivity in controlled cohorts. However, variability in viral load, sample handling, and storage conditions can significantly influence outcomes. Comprehensive field validation, including sensitivity, specificity, positive predictive value (PPV), and negative predictive value (NPV) across diverse populations, is still required before widespread clinical implementation.<sup>4,9,156</sup>

Fabiani *et al.* developed a smartphone-assisted  $\mu$ PADs for SARS-CoV-2 diagnosis and demonstrated that paper-based formats could deliver sensitive results suitable for large-scale screening.<sup>142</sup> Similarly, Tsai *et al.* and Bhardwaj *et al.* described the development of paper-based devices capable of detecting TB and influenza, respectively.<sup>73,190</sup>

While these devices offer high clinical and public health value, their performance is often evaluated under controlled lab settings. There is a clear need for real-world validation studies, particularly in resource-limited or community settings, where they are most needed. Moreover, integration with smartphone-based image analysis and connectivity tools could enhance the impact of these technologies, enabling real-time epidemiological monitoring.

It is important to highlight that saliva contains nucleases, mucins, and enzymes that may degrade viral components. Without integrated sample preparation steps, such as thermal lysis, filtering membranes, or pH stabilization, the sensitivity and reliability of these tests decline. Designs like those developed by Bhardwaj *et al.*, which incorporate on-paper heating zones and lyophilized reagents, pave the way for more robust field use.<sup>190</sup>

**5.2.6 Drugs and toxic substances.** In forensic and clinical toxicology, confirmatory analysis is typically performed using GC-MS or LC-MS/MS analysis, which provide high selectivity and legally defensible results.  $\mu$ PADs developed for detecting drugs of abuse, such as methamphetamines, ethanol, and opioids, have progressed rapidly, particularly in forensic screening and emergency diagnostics. Recent examples include devices that demonstrated saliva-based detection of opioids and ethanol with excellent portability and user-friendly operation.<sup>148,192,193</sup>

Although several strategies employing pre-treatment layers, filtration steps, or selective reagents have shown promise, significant challenges remain. Issues such as limited selectivity, false-positive responses, and matrix interference continue to affect analytical reliability. Further advances are required to establish standardized cut-off values, improve quantification

accuracy, and minimize interference from endogenous salivary components.<sup>193,203</sup>

### 5.3 Strategies to overcome salivary matrix challenges

Since salivary diagnostics can be affected by pre-analytical factors, such as viscosity fluctuations, dilution effects, enzymatic degradation, mucin-associated matrix interference, and the low abundance of clinically relevant biomarkers, the rational design of  $\mu$ PADs can mitigate these constraints by incorporating sample conditioning into the device architecture and enabling on-site saliva analysis.<sup>23,44,106</sup>

The porous cellulose matrix acts as a passive filtration layer, retaining larger particulates and mucin aggregates during capillary flow. Flow regulation further helps mitigate salivary variability.<sup>4,204</sup> Channel geometry, multilayer configurations, and embedded delay elements enable modulation of reaction timing and fluid transport. When combined with previously discussed valve systems and 3D  $\mu$ PAD architectures, these approaches allow sequential reactions and improved reproducibility under heterogeneous viscosity conditions.

Integration of sample treatment within hybrid systems also strengthens analytical robustness. Liu *et al.* reported a centrifugal microfluidic disc coupled with  $\mu$ PAD detection for salivary SARS-CoV-2 nucleocapsid protein, achieving efficient on-disc sample conditioning and low detection limits (10 pg mL<sup>-1</sup>) with performance comparable to that of commercial lateral flow assays.<sup>205</sup> This illustrates how mechanical preprocessing and paper-based sensing can be combined synergistically to address the complexity of the salivary matrix.

In addition, reagent immobilization and surface functionalization strategies enhance stability and selectivity. Although often demonstrated in urine-based devices, such as the enzymatic nitrate  $\mu$ PAD developed by Ferreira *et al.*, these principles are directly translatable to saliva, where enzyme stabilization and controlled activation are critical for reproducible performance.<sup>194</sup> These examples demonstrate that  $\mu$ PADs can integrate pre-analytical control into their structural design, strengthening the link between analytical architecture and real-world salivary diagnostics.

### 5.4 Clinical validation and cohort-based studies

While a substantial portion of the literature on salivary  $\mu$ PADs remains centered on analytical optimization, many platforms still rely predominantly on simulated saliva to demonstrate performance.<sup>61,170,190</sup> These studies are essential for defining sensing mechanisms, calibration behavior, and matrix compatibility, thereby establishing the analytical foundation of the field. However, they do not directly address translational applicability in clinically characterized populations.

$\mu$ PADs for salivary analysis have begun to be evaluated in real saliva samples, although typically in modest cohorts (often  $n < 20$  per group).<sup>55,173,194</sup> Santana-Jiménez *et al.*, for example, demonstrated the feasibility of a bienzymatic paper-based glucose sensor applied directly to untreated saliva.<sup>206</sup> Ferreira *et al.* reported the successful determination of nitrate and nitrite in saliva with verification using reference

methods,<sup>167</sup> and Kumar *et al.* validated a phosphate  $\mu$ PAD in 19 saliva samples with good correlation to spectrophotometric analysis.<sup>173</sup> In most cases, the primary objective was to demonstrate the applicability of the device using authentic samples rather than statistically powered clinical validation, and diagnostic cut-offs, sensitivity, and specificity metrics remain largely undefined.

Importantly, the clinical maturity of salivary biomarkers varies depending on the pathology under investigation. For systemic conditions, cohort-based validation of salivary markers remains limited and heterogeneous.<sup>4,5</sup> In contrast, for localized inflammatory diseases, such as periodontitis, salivary biomarkers have been more consistently studied in stratified patient populations.<sup>6,11,12,18</sup> Bezerra Júnior *et al.* reported significant alterations in organic and inorganic salivary compounds in individuals with chronic periodontal disease, supporting the biological plausibility of saliva-based assessment.<sup>207</sup> Similarly, Almeida *et al.* evaluated salivary cortisol in individuals with temporomandibular disorders within a clinically characterized cohort, illustrating that biomarker investigation in saliva predates device-oriented validation.<sup>208</sup>

Taken together, these findings reveal an asymmetry in the literature: while several salivary biomarkers have undergone cohort-based clinical investigation,  $\mu$ PAD-based validation in comparable populations remains at an early stage. The field is clearly shifting from analytical proof-of-concept to translational evaluation, yet convergence between biomarker clinical evidence and large-scale device validation remains needed. Statistically powered, multicenter studies will be essential to consolidate salivary  $\mu$ PADs as robust diagnostic tools, particularly for systemic diseases.<sup>209–211</sup>

### 5.5 Current limitations and translational challenges

Despite the remarkable advances discussed throughout this review, several limitations still hinder the full clinical translation of salivary  $\mu$ PADs. One major concern is the long-term stability and shelf-life of functionalized paper substrates, particularly in enzyme-based and nanoparticle-modified systems, where humidity, temperature fluctuations, and oxidation may compromise analytical performance.<sup>4–8</sup>

In addition, batch-to-batch variability arising from differences in paper porosity, fiber distribution, surface treatments, and manual reagent deposition can significantly affect reproducibility, especially in quantitative applications. Pre-analytical variability also represents a critical barrier: saliva composition is influenced by hydration status, circadian rhythm, stimulation conditions, and collection protocols, yet these factors are not consistently standardized across studies.<sup>12</sup>

Although numerous proof-of-concept devices have been reported, large-scale clinical validation studies directly comparing  $\mu$ PADs with gold-standard laboratory techniques remain limited. Addressing these challenges will require standardized fabrication workflows, harmonized saliva collection protocols, stability studies under real-world conditions, and statistically powered clinical evaluations to ensure regulatory acceptance and real-world implementation.

## 6. Future perspectives

Compared to blood, urine, or other bodily fluids, saliva is considered to be stable and easy to handle, but it exhibits dynamic behavior depending on the individual and their own habits. Saliva is ideal for field testing and is highly suitable for POC applications. In this section, the trends in saliva testing using  $\mu$ PADs will be discussed, focusing on portable and digital transducers, as well as wearable sensors and devices that can be further integrated into the *Internet of Things* (IoT) framework. We will also discuss the emerging sensing strategies used for the detection and prediction of various human diseases.

### 6.1 Integration with digital technologies

IoT technologies have introduced a new frontier of POC analytical devices, enabling more integrated, accessible, and decentralized diagnostic solutions.<sup>212</sup> Among IoT tools, smartphones stand out as particularly versatile platforms, as they are equipped with a range of sensors, actuators, and communication modules that enable real-time data acquisition, processing, and transmission.<sup>212–214</sup> While colorimetric detection on  $\mu$ PADs can be readily performed using a standard smartphone camera, electrochemical detection typically requires the use of a potentiostat. In response to this need, the development of portable and open-source potentiostats has gained significant momentum in recent years, particularly following the publication of several pioneering studies that have demonstrated their feasibility and effectiveness in resource-limited settings.<sup>214</sup>

Portable and miniaturized potentiostats were initially developed for coupling with portable devices for sweat analysis and opening the door to non-invasive and continuous analysis of body fluid samples.<sup>212–218</sup> This innovation has catalyzed the development of various handheld and open-source potentiostats, such as those offered by PalmSens and Io-Rodeo, as well as low-cost custom devices reported in academic research. For instance, Anshori *et al.* designed a low-cost, portable potentiostat (USD 21.4) that supports multiple electrochemical techniques, including CV, LSV, SWV, DPV, NPV, and chronoamperometry, with a performance comparable to that of commercial systems (average accuracy >90% *vs.* EmStat Pico). Notably, it also enables semi-parallel analysis using three simultaneous channels.<sup>218</sup>

Particularly for salivary analysis, the use of a portable, battery-powered, and wireless potentiostat is highly desired, especially in POC applications. As demonstrated by Bianchi *et al.*, the integration of a potentiostat into IoT-based biosensor systems enables autonomous operation and cloud-based data processing, a feature that is critical for decentralized diagnostics.<sup>212</sup> Their device operates independently without the need for smartphones or PCs, offering Wi-Fi connectivity and machine learning-based calibration directly through a web interface. Similarly, Ferreira *et al.* developed the PULSE system, a fast and miniaturized platform for lab-on-site electrochemistry, capable of performing chronoamperometry

and cyclic voltammetry with high accuracy (97.6%) and rapid pH detection in just 2 s, emphasizing its utility in real-time analysis.<sup>217</sup>

Although none of these devices were initially designed for saliva analysis, their performance demonstrated in real biological matrices (*e.g.*, sweat, blood, or artificial fluids) positions them as powerful candidates for adaptation. However, due to saliva's complex matrix and potential interferences, as well as its enzymatic activity, any such adaptation must consider strategies such as microfluidic separation or selective membrane integration. These adaptations are essential to preserve signal stability and ensure accurate biomarker detection. Moreover, the implementation of IoT features, such as real-time data upload, wireless communication, and AI-assisted interpretation, represents a crucial step for smart diagnostics, particularly under emergency health scenarios such as the COVID-19 pandemic.<sup>212,218</sup> While wearable electrochemical sensors have progressed notably for sweat monitoring, similar systems for saliva remain a frontier yet to be fully explored—one that demands miniaturization, biofouling prevention, and real-time data transmission.

These technological advances also position IoT-integrated  $\mu$ PAD systems within the contemporary REASSURED framework for point-of-care diagnostics.<sup>219,220</sup> Originally defined as ASSURED and later expanded to incorporate real-time connectivity and ease of specimen collection, this framework reflects the evolution of decentralized testing toward digitally connected and minimally invasive platforms.<sup>221</sup> In this context, the combination of salivary sampling with portable readout, wireless communication, and cloud-based processing directly addresses multiple REASSURED dimensions, extending beyond affordability and user-friendliness to include connectivity-driven data integration.<sup>221–223</sup> Such alignment enhances the potential of  $\mu$ PAD-based systems for large-scale screening, longitudinal monitoring, and integration into digital health infrastructures, ultimately strengthening their contribution to clinical decision-making and real-time public health surveillance.

However, achieving full decentralization requires not only digital connectivity but also operational autonomy. While IoT-enabled  $\mu$ PADs address data transmission and integration, the dependence on external power sources still limits their deployment in resource-constrained or remote settings. In this context, self-powered  $\mu$ PADs emerge as a complementary strategy aimed at eliminating energy dependency and enabling fully autonomous analytical platforms.

### 6.2 Toward fully autonomous and self-powered $\mu$ PAD platforms

Self-powered  $\mu$ PADs represent an emerging strategy to achieve fully autonomous analytical platforms by integrating fluid handling and energy generation within the same device architecture.<sup>222,223</sup> In paper-based systems, autonomous operation is intrinsically facilitated by capillary microfluidics, which leverages physical forces such as surface tension, viscosity, and pressure gradients to drive fluid flow, without exter-

nal pumps, to control timing, directionality, and flow rates.<sup>224,225</sup>

Demonstrations of self-powered sensors were provided by Fischer *et al.*, who developed a 3D origami enzymatic fuel cell in which glucose oxidation generated the analytical current directly within the sensor, eliminating the need for external power sources.<sup>225</sup> Similarly, Pal *et al.* integrated a triboelectric generator, enabling user-activated energy harvesting to power quantitative sensing.<sup>226</sup> A particularly relevant advancement for salivary diagnostics on paper was demonstrated by Mohammadifar and Choi, who reported a saliva-activated paper biobattery based on lyophilized exoelectrogenic bacteria preinoculated onto paper.<sup>227</sup> Upon rehydration with a single drop of saliva, the microbial fuel cells generated electrical power within minutes, sufficient to drive on-chip electronics. The freeze-dried bacteria enabled extended shelf life, while series integration of multiple cells on a single paper sheet enhanced power output. This work highlights the feasibility of saliva not only as a diagnostic fluid but also as a direct energy trigger, reinforcing the concept of fully autonomous, disposable paper-based platforms for point-of-care applications.

### 6.3 Wearable devices and saliva collection

Saliva is an attractive biofluid for diagnostics due to its non-invasive, stress-free collection, which can be self-performed with minimal training. Despite these advantages, saliva analysis demands careful collection to avoid interference from food debris, blood traces, and oral bacteria, especially for low-concentration biomarkers.<sup>163,228,229</sup> Currently, there are no standardized methods, and commercial tools include swabs, funnels, dried spot cards, and passive drool collectors. Dried spot methods, using materials such as Whatman 903 cards, are especially suitable for  $\mu$ PADs, as they handle small volumes (10–100  $\mu$ L). For more precise sampling, devices like the Lashley cup target saliva from the parotid duct.<sup>4,100,145</sup>

Wearable saliva sensors are particularly promising for continuous biomarker monitoring.<sup>71</sup> Although paper has not yet been extensively employed as the core sensing element in wearable saliva platforms, particularly those designed for continuous or real-time monitoring, it remains a highly promising material. Its intrinsic biocompatibility, natural absorptive capacity, low cost, disposability, and compatibility with both colorimetric and electrochemical detection methods make paper an attractive option for the development of lightweight, flexible, and user-friendly wearable systems. Rather than competing with existing materials, paper-based architectures may offer complementary advantages that can be strategically leveraged in future wearable saliva biosensing technologies.

Fig. 7 illustrates representative devices in this category. Among these, Arakawa *et al.* introduced a mouthguard biosensor in which cellulose acetate functions as a selective filtration membrane rather than as the sensing element itself, effectively reducing interference from salivary constituents such as uric and ascorbic acids and thereby improving the specificity of electrochemical glucose detection (Fig. 7).<sup>229</sup>

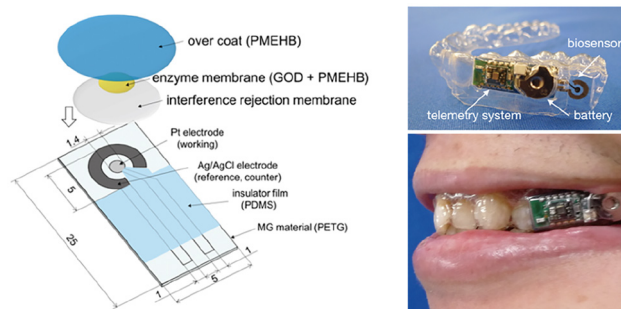


Fig. 7 Example of a wearable saliva-based diagnostic device: cellulose acetate-coated mouthguard biosensor for *in vivo* salivary glucose monitoring with interference rejection. Reprinted from Arakawa *et al.*,<sup>229</sup> with permission.

### 6.4 Emerging biomarkers

Recently, there has been increasing interest in identifying emerging biomarkers in saliva for the detection of systemic illnesses, neurological diseases, cancers, and stress. A particularly promising area of research involves the development of methods for detecting extracellular vesicles (EVs), which are crucial for understanding human health. EVs are lipid bilayer entities involved in cellular communication and can be used to diagnose and monitor a range of conditions, including periodontal diseases, oral cancer, primary Sjögren's syndrome, and neurological disorders.<sup>229</sup> These vesicles are secreted by various cell types and can be found in blood, urine, and saliva. Among EVs, exosomes (30–150 nm in diameter) are especially useful as biomarkers due to their role in disease monitoring and their protective structure, which safeguards their contents from degradation by exogenous enzymes and harsh environmental conditions. Exosomes carry valuable biomolecules, including soluble and membrane proteins, RNA, and DNA.

In recent years, paper has been employed to design portable and cost-effective devices for exosome analysis. Analytical techniques, such as lateral flow assays,<sup>229</sup> luminescence resonance energy transfer,<sup>230</sup> and distance-based assays, have been used to detect exosomes by targeting cluster differentiation (CD) molecules present on their membrane.<sup>231</sup> The distance-based assay, for example, detects exosome aggregation with polydiacetylene particles and analyzes solvent migration visually. While these methods provide useful insights into exosome identity, the detection of nucleic acids within exosomes, such as miRNA, has gained attention for its potential in early cancer detection and screening. Guo *et al.* proposed a pen-based paper chip for detecting breast-cancer-derived exosomal miRNA-21.<sup>232</sup> Despite these advances, the use of  $\mu$ PADs for exosome detection in saliva samples remains underexplored. There is still a need for protocols that address sample preparation, exosome separation, and detection for effective analysis in clinical applications.

### 6.5 Standardization and regulatory pathways

Despite significant technological progress in  $\mu$ PAD-based salivary diagnostics, translating laboratory prototypes into clinical

cally approved devices remains challenging. One of the primary barriers is the lack of standardized protocols for collecting, storing, and processing saliva. Variability in sampling methods (*e.g.*, stimulated *vs.* unstimulated saliva), circadian fluctuations, and differences in biomarker concentration ranges make inter-study comparisons difficult and hinder large-scale validation.<sup>2–6</sup>

In addition, reproducibility in device fabrication, including paper batch variability, reagent immobilization consistency, and storage stability, must be addressed to ensure analytical robustness.<sup>12</sup> Establishing standardized performance metrics (limit of detection, sensitivity, specificity, and clinical agreement with reference methods) is essential for regulatory approval and for meaningful comparison across platforms.<sup>13,23</sup>

From a regulatory perspective,  $\mu$ PAD-based diagnostic devices must comply with regional frameworks, such as FDA clearance in the United States or CE marking under the European *In Vitro* Diagnostic Regulation (IVDR). The recent COVID-19 pandemic highlighted the strategic importance of rapid, scalable diagnostic platforms, many of which relied on paper-based lateral flow technologies as foundational tools for mass screening.<sup>16</sup> These devices demonstrated how simplified microfluidic architectures can successfully transition from laboratory research to large-scale deployment when aligned with regulatory pathways and manufacturing scalability.<sup>15,21,41</sup>

Indeed, paper-based diagnostics are not conceptually new to clinical practice. The commercial pregnancy test, one of the most successful diagnostic tools worldwide, relies on a paper-based microfluidic format combined with colorimetric detection, offering simplicity, robustness, reproducibility, and low cost. Its widespread adoption illustrates how paper-based technologies can achieve regulatory approval, market penetration, and sustained societal impact when supported by clear clinical need and standardized validation processes.<sup>16,37,41</sup>

Bridging the gap between academic innovation and regulatory compliance will therefore require early integration of quality control, clinical validation, and manufacturing considerations during device development. Interdisciplinary collaboration among chemists, clinicians, engineers, regulatory specialists, and industry partners will be essential to transform promising  $\mu$ PAD prototypes into reliable, scalable, and clinically approved diagnostic tools.

## 7. Conclusions

Paper-based microfluidic devices have undergone significant advancements, evolving from rudimentary platforms that relied on simple color strip detection into sophisticated lab-on-a-chip systems. These improvements have been largely driven by developments in microtechnology, enabling the adoption of high-precision techniques such as photolithography—once restricted to cleanroom environments—and later transitioning to more accessible fabrication methods using portable tools, including manual printers, syringes, thermal laminators, and even repurposed children's toys. This adapta-

bility has granted unprecedented versatility, positioning such platforms as powerful tools for clinical diagnostics, especially in resource-limited settings and point-of-care applications.

As the demand for non-invasive diagnostic methods has grown,  $\mu$ PADs have been increasingly explored for salivary analysis. As highlighted in this review, saliva contains a wide range of biomarkers—proteins, hormones, enzymes, metabolites, microRNAs, and electrolytes—that reflect systemic physiological and pathological states, making it highly suitable for diagnosing conditions such as cancer, viral infections, metabolic disorders, cardiovascular diseases, and oral health issues.

Salivary diagnostics through paper-based devices align strongly with the ASSURED criteria established by the WHO for global health diagnostics. More recently, the evolution toward the REASSURED framework further strengthens the relevance of IoT-integrated and saliva-based  $\mu$ PAD platforms within contemporary decentralized healthcare models. The convergence of accessible technology and urgent clinical needs makes  $\mu$ PADs a promising solution for frontline healthcare services and emergency health scenarios, particularly in underserved regions.

While some salivary biomarkers—such as lactoferrin, cortisol, and amylase—are already well-established, many others remain a “black box,” requiring more precise screening and robust clinical validation. Developing a clearer correlation between conventional diagnostic methods and disease-specific biomarkers is essential to fully realize the potential of  $\mu$ PADs in early disease detection.

Furthermore, the multiplexed detection of several biomarkers in a single sample—for example, in the diagnosis of cancer, diabetes, kidney disorders, and periodontal disease—has enabled more accurate and sensitive diagnostics. Nevertheless, significant challenges remain, including the standardization of biomarker concentrations, the integration of sample pre-treatment steps (*e.g.*, filtration, extraction, and concentration) into a single device, the development of truly standalone devices independent of smartphones or external readers, and mitigating interference from biological components in complex samples. Multiplexed bioanalysis and the advancement of highly specific and sensitive sensors represent promising directions to enhance the reliability of  $\mu$ PADs in real-world clinical samples.

With continuous innovation in functional materials, microfabrication, and device miniaturization, paper-based analytical technologies are expected to play an increasingly central role in democratizing early diagnosis and advancing global public health. In parallel, the growing maturity of salivary diagnostics on  $\mu$ PADs opens up promising avenues for commercialization, especially as they offer a low-cost, user-friendly alternative to conventional lab diagnostics. Their portability, simplicity, and ability to deliver rapid results make them particularly attractive for direct-to-consumer applications, home testing kits, and telehealth integration. When coupled with digitally connected infrastructures, these platforms may support scalable screening programs, longitudinal monitoring, and real-time data-

driven clinical decision-making, consolidating their position within the REASSURED paradigm of modern POCT. As regulatory pathways become clearer and manufacturing scalability improves, these devices hold significant potential to disrupt traditional diagnostic markets and expand access to personalized, preventive healthcare worldwide.

## Author contributions

Lucas R. Sousa: conceptualization, formal analysis, investigation, methodology, visualization, and writing – original draft. Larissa G. Velasco: conceptualization, formal analysis, investigation, methodology, visualization, and writing – original draft. Sandra G. Vlachovsky: conceptualization, formal analysis, investigation, methodology, visualization, and writing – original draft. Federico Figueredo: conceptualization, supervision, and writing – review and editing. Eduardo Cortón: conceptualization, supervision, and writing – review and editing. Wendell K. T. Coltro: conceptualization, funding acquisition, project administration, supervision, and writing – review and editing.

## Conflicts of interest

There are no conflicts to declare.

## Data availability

No primary research results, software or code have been included, and no new data were generated or analysed as part of this review.

## Acknowledgements

The authors would like to thank the CNPq (grants 308136/2025-0 and 406309/2025-6), the CONICET, the National Agency of Scientific and Technological Promotion (ANPCyT) (grant BID-PICT 2020-04023), and the INCTBio (grant 408338/2024-5) for the financial support, scholarships, and research fellowships.

## References

- 1 Y. F. Shang, Y. Y. Shen, M. C. Zhang, M. C. Lv, T. Y. Wang, X. Q. Chen and J. Lin, *Front. Endocrinol.*, 2023, **14**, 1061235.
- 2 A. M. Chibly, M. H. Aure, V. N. Patel and M. P. Hoffman, *Physiol. Rev.*, 2022, **102**, 1495–1552.
- 3 A. Riva, *J. Anat.*, 2010, **217**, 755–756.
- 4 T. W. Pittman, D. B. Decsi, C. Punyadeera and C. S. Henry, *Theranostics*, 2023, **13**, 1091–1108.
- 5 S. P. Humphrey and R. T. Williamson, *J. Prosthet. Dent.*, 2001, **85**, 162–169.
- 6 G. B. Proctor, *Periodontol. 2000*, 2016, **70**, 11–25.
- 7 T. A. Nguyen, R. H. Chen, B. A. Hawkins, D. E. Hibbs, H. Y. Kim, N. J. Wheate, P. W. Groundwater, S. L. Stocker and J.-W. C. Alffenaar, *Clin. Pharmacokinet.*, 2024, **63**, 1067–1087.
- 8 G. B. Proctor and G. H. Carpenter, *Auton. Neurosci.*, 2007, **133**, 3–18.
- 9 R. M. Nagler, *Clin. Chem.*, 2008, **54**, 1415–1417.
- 10 T. Sri Santosh, R. Parmar, H. Anand, K. Srikanth and M. Saritha, *Cureus*, 2020, **12**, e7708.
- 11 H. Mortazavi, A.-A. Yousefi-Koma and H. Yousefi-Koma, *BMC Oral Health*, 2024, **24**, 168.
- 12 A. Sheini, *Microchim. Acta*, 2020, **187**, 565.
- 13 N. Sritong, M. Sala de Medeiros, L. A. Basing and J. C. Linnes, *Lab Chip*, 2023, **23**, 888–912.
- 14 M. M. Bordbar, H. Samadinia, A. Sheini, J. Aboonajmi, H. Sharghi, P. Hashemi, H. Khoshshafar, M. Ghanei and H. Bagheri, *Talanta*, 2022, **246**, 123537.
- 15 G. Ji, J. Wang, Z. Wang, S. Zhang, Z. Fang, Y. Wang and Z. Gao, *Biosens. Bioelectron.*, 2024, **261**, 116509.
- 16 T. Akyazi, L. Basabe-Desmonts and F. Benito-Lopez, *Anal. Chim. Acta*, 2018, **1001**, 1–17.
- 17 A. B. Anushka and P. K. Das, *Eur. Phys. J. Spec. Top.*, 2023, **232**, 781–815.
- 18 J. C. Leão, M. A. Santos, R. Valdivieso and L. C. Brazaca, *J. Dent. Res.*, 2025, **104**, 123–135.
- 19 V.-T. Nguyen, S. Song, S. Park and C. Joo, *Biosens. Bioelectron.*, 2020, **152**, 112015.
- 20 S.-G. Jeong, J. Kim, S. H. Jin, K.-S. Park and C.-S. Lee, *Korean J. Chem. Eng.*, 2016, **33**, 2761–2770.
- 21 A. Rubio-Monterde, D. Quesada-González and A. Merkoçi, *Anal. Chem.*, 2023, **95**, 468–489.
- 22 R. M. Roller and M. Lieberman, *Sens. Actuators. B. Chem.*, 2023, **392**, 134059.
- 23 K. Yamada, T. G. Henares, K. Suzuki and D. Citterio, *Angew. Chem., Int. Ed.*, 2015, **54**, 5294–5310.
- 24 P. Spicar-Mihalic, B. Toley, J. Houghtaling, T. Liang, P. Yager and E. Fu, *J. Micromech. Microeng.*, 2013, **23**, 067003.
- 25 X. Fang, S. Wei and J. Kong, *Lab Chip*, 2014, **14**, 911.
- 26 H. Asano and Y. Shiraishi, *Anal. Chim. Acta*, 2015, **883**, 55–60.
- 27 E. W. Nery and L. T. Kubota, *Anal. Bioanal. Chem.*, 2013, **405**, 7573–7595.
- 28 N. F. Prebianto and A. D. Futra, in *2018 International Conference on Applied Engineering (ICAE)*, IEEE, 2018, pp. 1–5.
- 29 M. A. Hegener, H. Li, D. Han, A. J. Steckl and G. M. Pauletti, *Biomed. Microdevices*, 2017, **19**, 64.
- 30 G. He, T. Dong, Z. Yang, A. Branstad, L. Huang and Z. Jiang, *Analyst*, 2022, **147**, 1273–1293.
- 31 R. H. Tang, H. Yang, J. R. Choi, Y. Gong, S. S. Feng, B. Pingguan-Murphy, Q. S. Huang, J. L. Shi, Q. B. Mei and F. Xu, *Crit. Rev. Biotechnol.*, 2017, **37**, 411–428.

- 32 C. Wang, M. Liu, Z. Wang, S. Li, Y. Deng and N. He, *Nano Today*, 2021, **37**, 101092.
- 33 J. R. Mejía-Salazar, K. R. Cruz, E. M. M. Vásques and O. N. Oliveira Jr., *Sensors*, 2020, **20**, 1951.
- 34 S. Rink and A. J. Baeumner, *Anal. Chem.*, 2023, **95**, 1785–1793.
- 35 A. F. Abdallah, A. Z. Mohamed, A. Siddiqui, *et al.*, *Sci. Rep.*, 2025, **15**, 31872.
- 36 S. M. Khan, J. M. Nassar and M. M. Hussain, *ACS Appl. Electron. Mater.*, 2021, **3**, 30–52.
- 37 A. W. Martinez, S. T. Phillips, M. J. Butte and G. M. Whitesides, *Angew. Chem.*, 2007, **119**, 1340–1342.
- 38 S. Nishat, A. T. Jafry, A. W. Martinez and F. R. Awan, *Sens. Actuators. B. Chem.*, 2021, **336**, 129681.
- 39 A. Lomae, P. Preechakasedkit, K. Teekayupak, Y. Panraksa, J. Yukird, O. Chailapakul and N. Ruecha, *Curr. Top. Med. Chem.*, 2022, **22**, 2282–2313.
- 40 T. M. Blicharz, D. M. Rissin, M. Bowden, R. B. Hayman, C. DiCesare, J. S. Bhatia, N. Grand-Pierre, W. L. Siqueira, E. J. Helmerhorst, J. Loscalzo, F. G. Oppenheim and D. R. Walt, *Clin. Chem.*, 2008, **54**, 1473–1480.
- 41 P. W. Smit, I. Elliott, R. W. Peeling, D. Mabey and P. N. Newton, *Am. J. Trop. Med. Hyg.*, 2014, **90**, 195–210.
- 42 T. Thongkam and K. Hemavibool, *Microchem. J.*, 2020, **159**, 105412.
- 43 L. R. Sousa, H. A. Silva-Neto, P. P. E. Campos, G. F. Duarte-Junior, I. Medeiros Junior, R. M. Carvalho and W. K. T. Coltro, *Microchem. J.*, 2022, **183**, 108024.
- 44 N. S. Moreira, K. M. P. Pinheiro, L. R. Sousa, G. D. S. Garcia, F. Figueredo and W. K. T. Coltro, *Anal. Methods*, 2024, **16**, 33–39.
- 45 C. Lu, S. Xu, S. Wang, T. Wang, W.-L. Wang, C. Yang and Y. Zhang, *Anal. Chem.*, 2024, **96**, 2387–2395.
- 46 F. G. Bellagambi, T. Lomonaco, P. Salvo, F. Vivaldi, M. Hangouët, S. Ghimenti, D. Biagini, F. Di Francesco, R. Fuoco and A. Errachid, *TrAC, Trends Anal. Chem.*, 2020, **124**, 115781.
- 47 Y. Sun, Q. Jiang, F. Chen and Y. Cao, *Electrochem. Sci. Adv.*, 2022, **2**, e2100057.
- 48 T. Ozer, C. McMahon and C. S. Henry, *Annu. Rev. Anal. Chem.*, 2020, **13**, 85–109.
- 49 D. M. Cate, J. A. Adkins, J. Mettakoonpitak and C. S. Henry, *Anal. Chem.*, 2015, **87**, 19–41.
- 50 D. L. Clegg, *Anal. Chem.*, 1950, **22**, 48–59.
- 51 T. H. Jupille and J. A. Perry, *CRC Crit. Rev. Anal. Chem.*, 1977, **6**, 325–359.
- 52 S. M. Partridge, *Nature*, 1946, **158**, 270–271.
- 53 G. O. da Silva, W. R. de Araujo and T. R. L. C. Paixão, *Talanta*, 2018, **176**, 674–678.
- 54 L. R. Sousa, B. G. S. Guinati, L. I. L. Maciel, T. A. Baldo, L. C. Duarte, R. M. Takeuchi, R. C. Faria, B. G. Vaz, T. R. L. C. Paixão and W. K. T. Coltro, *Lab Chip*, 2024, **24**, 467–479.
- 55 L. R. Sousa, H. A. Silva-Neto, L. F. Castro, K. A. Oliveira, F. Figueredo, E. Cortón and W. K. T. Coltro, *Anal. Bioanal. Chem.*, 2023, **415**, 4391–4400.
- 56 R. Tang, M. Y. Xie, M. Li, L. Cao, S. Feng, Z. Li and F. Xu, *Appl. Mater. Today*, 2022, **26**, 101305.
- 57 R. H. Tang, M. Li, L. N. Liu, S. F. Zhang, N. Alam, M. You, Y. H. Ni and Z. D. Li, *Cellulose*, 2020, **27**, 3835–3846.
- 58 A. W. Martinez, S. T. Phillips, B. J. Wiley, M. Gupta and G. M. Whitesides, *Lab Chip*, 2008, **8**, 2146.
- 59 D. Lee, T. Ozkaya-Ahmadov, C.-H. Chu, M. Boya, R. Liu and A. F. Sarioglu, *Sci. Adv.*, 2021, **7**, eabf9833.
- 60 C. Carrell, A. Kava, M. Nguyen, R. Menger, Z. Munshi, Z. Call, M. Nussbaum and C. Henry, *Microelectron. Eng.*, 2019, **206**, 45–54.
- 61 S. A. Bhakta, R. Borba, M. Taba, C. D. Garcia and E. Carrilho, *Anal. Chim. Acta*, 2014, **809**, 117–122.
- 62 S. Hyung, G. Karima, K. Shin, K. S. Kim and J. W. Hong, *BioChip J.*, 2021, **15**, 252–259.
- 63 D. Lin, B. Li, L. Fu, J. Qi, C. Xia, Y. Zhang, J. Chen, J. Choo and L. Chen, *Microsyst. Nanoeng.*, 2022, **8**, 53.
- 64 R. Tang, N. Alam, M. Li, M. Xie and Y. Ni, *Carbohydr. Polym.*, 2021, **268**, 118259.
- 65 C. W. Choi, D. Hong and M.-G. Kim, *Biosens. Bioelectron.*, 2025, **271**, 116971.
- 66 S. Kim and M.-G. Kim, *Anal. Chem.*, 2025, **97**, 2707–2713.
- 67 S. Singh, M. R. Hasan, A. Jain, R. Pilloton and J. Narang, *Chemosensors*, 2023, **11**, 255.
- 68 I. Jang, K. E. Berg and C. S. Henry, *Sens. Actuators. B. Chem.*, 2020, **319**, 128240.
- 69 L. Gutiérrez-Gálvez, N. Seddaoui, L. Fiore, L. Fabiani, T. García-Mendiola, E. Lorenzo and F. Arduini, *ACS Sens.*, 2024, **9**, 4047–4057.
- 70 S. Kou, L. M. Peters and M. R. Mucalo, *Int. J. Biol. Macromol.*, 2021, **169**, 85–94.
- 71 L. F. de Castro, S. V. de Freitas, L. C. Duarte, J. A. C. de Souza, T. R. L. C. Paixão and W. K. T. Coltro, *Anal. Bioanal. Chem.*, 2019, **411**, 4919–4928.
- 72 Y. J. Chi, B. Ryu, S. Ahn and W.-G. Koh, *Sens. Actuators. B. Chem.*, 2023, **396**, 134601.
- 73 T.-T. Tsai, C.-Y. Huang, C.-A. Chen, S.-W. Shen, M.-C. Wang, C.-M. Cheng and C.-F. Chen, *ACS Sens.*, 2017, **2**, 1345–1354.
- 74 K. Khachornsakkul, F. J. Rybicki and S. Sonkusale, *Talanta*, 2023, **260**, 124538.
- 75 X. Li, J. Tian, T. Nguyen and W. Shen, *Anal. Chem.*, 2008, **80**, 9131–9134.
- 76 T. Songjaroen, W. Dungchai, O. Chailapakul and W. Laiwattanapaisal, *Talanta*, 2011, **85**, 2587–2593.
- 77 H. Moulahoum, F. Ghorbanizamani and S. Timur, *Anal. Chim. Acta*, 2024, **1306**, 342617.
- 78 R. Ghosh, S. Gopalakrishnan, R. Savitha, T. Renganathan and S. Pushpavanam, *Sci. Rep.*, 2019, **9**, 7896.
- 79 A. Silvestri, S. Vázquez-Díaz, G. Misia, F. Poletti, R. López-Domene, V. Pavlov, C. Zanardi, A. L. Cortajarena and M. Prato, *Small*, 2023, **19**, e2300163.
- 80 N. Komuro, S. Takaki, K. Suzuki and D. Citterio, *Anal. Bioanal. Chem.*, 2013, **405**, 5785–5805.

- 81 G. Yang, L. Xie, M. Mäntysalo, J. Chen, H. Tenhunen and L.-R. Zheng, *IEEE Trans. Inf. Technol. Biomed.*, 2012, **16**, 1043–1050.
- 82 W.-H. Liang, C.-H. Chu and R.-J. Yang, *Talanta*, 2015, **145**, 6–11.
- 83 A. Espinosa, J. Diaz, E. Vazquez, L. Acosta, A. Santiago and L. Cunci, *Talanta Open*, 2022, **6**, 100142.
- 84 T. Monju, M. Hirakawa, S. Kuboyama, R. Saiki and A. Ishida, *Sens. Actuators. B. Chem.*, 2023, **375**, 132886.
- 85 T. Pomili, P. Donati and P. P. Pompa, *Biosensors*, 2021, **11**, 443.
- 86 M. Levis, N. Kumar, E. Apakian, C. Moreno, U. Hernandez, A. Olivares, F. Ontiveros and J. J. Zartman, *Biomicrofluidics*, 2019, **13**, 024111.
- 87 K. Pungjunun, A. Yakoh, S. Chaiyo, N. Praphairaksit, W. Siangproh, K. Kalcher and O. Chailapakul, *Microchim. Acta*, 2021, **188**, 140.
- 88 X. Zhao, C. Cui, L. Ma, Z. Ding, J. Hou, Y. Xiao, B. Liu, B. Qi, J. Zhang, J. Wei and N. Hao, *Chem. Eng.*, 2024, **480**, 148245.
- 89 J. Nie, Y. Zhang, L. Lin, C. Zhou, S. Li, L. Zhang and J. Li, *Anal. Chem.*, 2012, **84**, 6331–6335.
- 90 J. Sitanurak, N. Fukana, T. Wongpakdee, Y. Thepchuay, N. Ratanawimarnwong, T. Amornsakchai and D. Nacapricha, *Talanta*, 2019, **205**, 120113.
- 91 H. A. Silva-Neto, J. C. Jaime, D. S. Rocha, L. F. Sgobbi and W. K. T. Coltro, *Anal. Chim. Acta*, 2024, **1297**, 342336.
- 92 S. A. Klasner, A. K. Price, K. W. Hoeman, R. S. Wilson, K. J. Bell and C. T. Culbertson, *Anal. Bioanal. Chem.*, 2010, **397**, 1821–1829.
- 93 J. Olkkonen, K. Lehtinen and T. Erho, *Anal. Chem.*, 2010, **82**, 10246–10250.
- 94 A. W. Martinez, S. T. Phillips and G. M. Whitesides, *Proc. Natl. Acad. Sci. U. S. A.*, 2008, **105**, 19606–19611.
- 95 H. Liu and R. M. Crooks, *J. Am. Chem. Soc.*, 2011, **133**, 17564–17566.
- 96 Q. Cao, B. Liang, T. Tu, J. Wei, L. Fang and X. Ye, *RSC Adv.*, 2019, **9**, 5674–5681.
- 97 C. Aksoy, I. van Kesteren, H. Zuilhof and G. I. J. Salentijn, *ACS Appl. Bio Mater.*, 2025, **8**, 5.
- 98 Y. Liu, N. Lan, J. Zhao, L. Kong and Z. Lu, *Langmuir*, 2025, **41**(49), 33629–33639.
- 99 A. Chaudhuri, V. Arya, C. Bakli and S. Chakraborty, *J. Chem. Phys.*, 2024, **161**, 184702.
- 100 J. Noiphung, M. P. Nguyen, C. Punyadeera, Y. Wan, W. Laiwattanapaisal and C. S. Henry, *Theranostics*, 2018, **8**, 3797–3807.
- 101 A. Foglio-Bonda, F. Pattarino and P. L. Foglio-Bonda, *Eur. Rev. Med. Pharmacol. Sci.*, 2014, **18**, 2988–2994.
- 102 E. Moreno, P. Kumar, R. O. Adansi, A. Rodriguez and V. Kumar, *Proc. ASME Fluids Eng. Div. Summer Meet.*, 2024, **2**, V002T06A004.
- 103 Y. Jiao, C. Du, L. Zong, X. Guo, Y. Han, X. Zhang, L. Li, C. Zhang, Q. Ju, J. Liu, H.-D. Yu and W. Huang, *Sens. Actuators. B. Chem.*, 2020, **306**, 127239.
- 104 J. Houghtaling, T. Liang, G. Thiessen and E. Fu, *Anal. Chem.*, 2013, **85**, 11201–11204.
- 105 E. A. Phillips, R. Shen, S. Zhao and J. C. Linnes, *Lab Chip*, 2016, **16**, 4230–4236.
- 106 C. Chen, L. Zhao, H. Zhang, X. Shen, Y. Zhu and H. Chen, *Anal. Chem.*, 2019, **91**, 5169–5175.
- 107 L. R. Sousa, N. S. Moreira, B. G. S. Guinati, W. K. T. Coltro, E. Cortón and F. Figueredo, *Talanta*, 2024, **277**, 126361.
- 108 X. Jiang and Z. H. Fan, *Annu. Rev. Anal. Chem.*, 2016, **9**, 203–222.
- 109 B. Rofman, R. Naddaf, M. Bar-Dolev, T. Gefen, N. Ben-Assa, N. Geva-Zatorsky and M. Bercovici, *Lab Chip*, 2022, **22**, 4511–4520.
- 110 E. Mollaie, S. Asiaei and H. Aryan, *Microfluid. Nanofluidics*, 2022, **26**, 88.
- 111 T. Gölceç, V. Kiliç and M. Şen, *Anal. Sci.*, 2021, **37**, 561–567.
- 112 J. I. S. Aguiar, A. O. S. S. Rangel and R. B. R. Mesquita, *Talanta Open*, 2023, **8**, 100254.
- 113 J. I. S. Aguiar, M. T. S. Silva, H. A. G. Ferreira, E. C. B. Pinto, M. W. Vasconcelos, A. O. S. S. Rangel and R. B. R. Mesquita, *Talanta Open*, 2022, **6**, 100135.
- 114 O. R. Chanu, R. Savitha, A. Kapoor, S. Gopalakrishnan, V. Karthik and S. Pushpavanam, *Sens. Imaging*, 2024, **25**, 16.
- 115 L. Hongtanee, S. Chaiyo, H. Wu and A. Yakoh, *Adv. Healthc. Mater.*, 2025, **14**, 2404320.
- 116 F. T. S. M. Ferreira, A. O. S. S. Rangel and R. B. R. Mesquita, *Biosensors*, 2025, **15**, 48.
- 117 X. Tong, G. Li, Q. Guo, J. Hu, B. Zhang, S. Liu, J. Guo and L. Zhang, *Microchim. Acta*, 2025, **192**, 20.
- 118 A. Scarsi, D. Pedone and P. P. Pompa, *Nanoscale Adv.*, 2023, **5**, 329–336.
- 119 K. Khachornsakkul, W. Dungchai and N. Pamme, *ACS Sens.*, 2022, **7**, 2410–2419.
- 120 A. A. G. Yoshikawa, S. F. Cardoso, L. B. Esalabão, I. C. Pinheiro, P. Valverde, G. Caminha, O. B. Romero, L. Medeiros, L. D. P. Rona and A. N. Pitaluga, *Mem. Inst. Oswaldo Cruz*, 2024, **119**, e230236.
- 121 D. Lee, T. Ozkaya-Ahmadov and A. F. Sarioglu, *Small*, 2023, **19**, e2208035.
- 122 D. Houtzager, S. Armenta, J. M. Herrero-Martínez and H. Martínez-Pérez-Cejuela, *Anal. Bioanal. Chem.*, 2024, **416**, 255–264.
- 123 C. Srisomwat, N. Bawornnithichaiyakul, S. Khonyoung, W. Tiyapongpattana, S. Butcha, N. Youngvises and O. Chailapakul, *Talanta*, 2024, **280**, 126770.
- 124 M. Tarara, P. D. Tzanavaras and G. Z. Tsogas, *Sensors*, 2022, **23**, 198.
- 125 M. Khan, B. Zhao, W. Wu, M. Zhao, Y. Bi and Q. Hu, *TrAC, Trends Anal. Chem.*, 2023, **162**, 117029.
- 126 M. D. Gholami, K. Guppy-Coles, S. Nihal, D. Langguth, P. Sonar, G. A. Ayoko, C. Punyadeera and E. L. Izake, *Talanta*, 2022, **248**, 123630.

- 127 Y. Fan, J. Li, Y. Guo, L. Xie and G. Zhang, *Measurement*, 2021, **171**, 108829.
- 128 N. Nuchtavorn, T. Rypar, L. Nejd, M. Vaculovicova and M. Macka, *TrAC, Trends Anal. Chem.*, 2022, **150**, 116581.
- 129 G. M. Fernandes, W. R. Silva, D. N. Barreto, R. S. Lamarca, P. C. F. Lima Gomes, J. F. d. S. Petrucci and A. D. Batista, *Anal. Chim. Acta*, 2020, **1135**, 187–203.
- 130 M. Fotouhi, S. Seidi, Y. Razeghi and S. Torfinezhad, *Anal. Chim. Acta*, 2024, **1287**, 342127.
- 131 J. Yang, G. Li, S. Chen, X. Su, D. Xu, Y. Zhai, Y. Liu, G. Hu, C. Guo, H. B. Yang, L. G. Occhipinti and F. X. Hu, *ACS Sens.*, 2024, **9**, 1945.
- 132 Z. Lu, M. Chen, T. Liu, C. Wu, M. Sun, G. Su, X. Wang, Y. Wang, H. Yin, X. Zhou, J. Ye, Y. Shen and H. Rao, *ACS Appl. Mater. Interfaces*, 2023, **15**, 7.
- 133 M. Bhaiyya, D. Panigrahi, P. Rewatkar and H. Haick, *ACS Sens.*, 2024, **9**, 9.
- 134 L. Bezinge, C. Shih, D. A. Richards and A. J. deMello, *Small*, 2024, **20**, 2401148.
- 135 H. A. Silva-Neto, I. V. S. Arantes, A. L. Ferreira, G. H. M. do Nascimento, G. N. Meloni, W. R. de Araujo, T. R. L. C. Paixão and W. K. T. Coltro, *TrAC, Trends Anal. Chem.*, 2023, **158**, 116893.
- 136 L. C. Faustino, J. P. C. Cunha, W. Cantanhêde, L. T. Kubota and E. T. S. Gerôncio, *Microchim. Acta*, 2023, **190**, 338.
- 137 Y. Wada, E. Totsune, Y. Mikami-Saito, A. Kikuchi, T. Miyata and S. Kure, *Mol. Genet. Metab. Rep.*, 2023, **35**, 100970.
- 138 E. Eksin and A. Erdem, *Microchem. J.*, 2024, **204**, 111128.
- 139 W. Diao, C. Zhou, Z. Zhang, Y. Cao, Y. Li, J. Tang and G. Liu, *ACS Sens.*, 2024, **9**, 4265–4276.
- 140 P. Gao, T. Kasama, J. Shin, Y. Huang and R. Miyake, *Biosensors*, 2022, **12**, 995.
- 141 L. F. de Lima, P. P. Barbosa, C. L. Simeoni, R. F. d. O. de Paula, J. L. Proença-Modena and W. R. de Araujo, *ACS Appl. Mater. Interfaces*, 2023, **15**, 58079–58091.
- 142 L. Fabiani, L. Fiore, S. Fillo, N. D'Amore, R. De Santis, F. Lista and F. Arduini, *Bioelectrochemistry*, 2024, **156**, 108619.
- 143 L. F. de Lima, A. L. Ferreira, G. H. M. do Nascimento, L. P. Cardoso, M. B. de Jesus and W. R. de Araujo, *Chem. Eng. J.*, 2024, **494**, 152885.
- 144 S. Cinti, N. Colozza, I. Cacciotti, D. Moscone, M. Polomoshnov, E. Sowade, R. R. Baumann and F. Arduini, *Sens. Actuators. B. Chem.*, 2018, **265**, 155–160.
- 145 S. E. Denny, S. S. Nazeer, S. T. T. Bindu, J. Nair and R. S. Jayasree, *J. Lumin.*, 2018, **203**, 696–701.
- 146 Y. Jung, J. Kim, O. Awofeso, H. Kim, F. Regnier and E. Bae, *Appl. Opt.*, 2015, **54**, 9183.
- 147 N. Achetib, K. Falkena, M. Swayambhu, M. C. G. Aalders and A. van Dam, *Sci. Rep.*, 2023, **13**, 3195.
- 148 G. G. Morbioli, T. Mazzu-Nascimento, A. M. Stockton and E. Carrilho, *Anal. Chim. Acta*, 2017, **970**, 1–22.
- 149 X. Qin, J. Liu, Z. Zhang, J. Li, L. Yuan, Z. Zhang and L. Chen, *TrAC, Trends Anal. Chem.*, 2021, **143**, 116371.
- 150 A. Isa, M. Gharibi, A. Cetinkaya and S. A. Ozkan, *Microchem. J.*, 2025, **212**, 113210.
- 151 D. Obino, M. Vassalli, A. Franceschi, A. Alessandrini, P. Facci and F. Viti, *Sensors*, 2021, **21**, 3058.
- 152 H. Haghgouei and N. Alizadeh, *Anal. Chim. Acta*, 2024, **1330**, 343275.
- 153 J. Mettakoonpitak, K. Boehle, S. Nantaphol, P. Teengam, J. A. Adkins, M. Srisa-Art and C. S. Henry, *Electroanalysis*, 2016, **28**, 1420–1436.
- 154 S. Chen, Q. Wan and A. K. Badu-Tawiah, *J. Am. Chem. Soc.*, 2016, **138**, 6356–6359.
- 155 P. Pandit, B. Crewther, C. Cook, C. Punyadeera and A. K. Pandey, *Mater. Adv.*, 2024, **5**, 5339–5350.
- 156 Y. Li, Y. Ou, K. Fan and G. Liu, *Theranostics*, 2024, **14**, 6969–6990.
- 157 H. Sobczak-Jaskow, B. Kochańska and B. Drogoszewska, *Medicina*, 2023, **59**, 1073.
- 158 C. Prakobdi, T. A. Baldo, P. Aryal, J. Link, P. Saetear and C. S. Henry, *Anal. Methods*, 2024, **16**, 2489–2495.
- 159 Y. Xia, J. Si and Z. Li, *Biosens. Bioelectron.*, 2016, **77**, 774–789.
- 160 E. F. M. Gabriel, P. T. Garcia, T. M. G. Cardoso, F. M. Lopes, F. T. Martins and W. K. T. Coltro, *Analyst*, 2016, **141**, 4749–4756.
- 161 P. Hernandez, M. Arredondo, N. Pineda, J. Campoy, R. Acevedo, X. Olvera, D. Romero and N. Batina, *Microfluid. Nanofluid.*, 2025, **29**, 59.
- 162 S. Lee, D. S. Kulyk, S. O. Afriyie, K. Badu and A. K. Badu-Tawiah, *Anal. Chem.*, 2022, **94**, 14377–14384.
- 163 B. Sun, X. Zhang, Y. Li and J. Wang, *Colloids Surf., B*, 2021, **205**, 111864.
- 164 T. Songjaroen, W. Dungchai, O. Chailapakul, C. S. Henry and W. Laiwattanapaisal, *Lab Chip*, 2012, **12**, 3392.
- 165 A. Vaquer, E. Barón and R. de la Rica, *ACS Sens.*, 2022, **7**, 488–494.
- 166 E. B. Aydın, M. Aydın and M. K. Sezginürk, *Sens. Actuators. B. Chem.*, 2023, **378**, 133208.
- 167 F. T. S. M. Ferreira, R. B. R. Mesquita and A. O. S. S. Rangel, *Talanta*, 2020, **219**, 121183.
- 168 C. Chen, B. Ran, B. Liu, Y. Xiao, G. Tang, T. Shen, J. Liang and Z. Liang, *Microchem. J.*, 2025, **210**, 112966.
- 169 M. Naseri, Z. M. Ziora, G. P. Simon and W. Batchelor, *Rev. Med. Virol.*, 2022, **32**, e2263.
- 170 M. D. M. Castro, H. M. Ismail, C. A. Montenegro-Quiñonez, E. I. Reipold, S. Shilton, C. Denking and S. Yerlikaya, *BMJ Open*, 2025, **15**, e092774.
- 171 S. S. Paramasivam, S. A. Mariappan, N. K. Sethy and P. Manickam, *Mater. Adv.*, 2023, **4**, 6223–6232.
- 172 S. R. Gaspar, L. Proença, R. Alves and M. G. Almeida, *Sens. Biosensing Res.*, 2025, **49**, 100860.
- 173 S. Kumar, P. Patra, S. R. Kumar, Rohit, A. Raj and M. Pathak, *Microchem. J.*, 2026, **221**, 116890.
- 174 V. Mazzaracchio, A. Sassolini, K. Y. Mitra, D. Mitra, G. M. Stojanović, A. Willert, E. Sowade, R. R. Baumann, R. Zichner, D. Moscone and F. Arduini, *Green Anal. Chem.*, 2022, **1**, 100006.

- 175 A. Soni, R. K. Surana and S. K. Jha, *Sens. Actuators. B. Chem.*, 2018, **269**, 346–353.
- 176 K. Fan, J. Zeng, C. Yang, G. Wang, K. Lian, X. Zhou, Y. Deng and G. Liu, *ACS Sens.*, 2022, **7**, 2073–2081.
- 177 X. Huang, W. Shi, J. Li, N. Bao, C. Yu and H. Gu, *Anal. Chim. Acta*, 2020, **1103**, 75–83.
- 178 H. Kudo, K. Maejima, Y. Hiruta and D. Citterio, *SLAS Technol.*, 2020, **25**, 47–57.
- 179 D. Alageswari, A. Lakshmi Devi, P. E. Resmi, P. V. Suneesh, A. Pradeep and T. G. Satheesh Babu, *J. Anal. Test.*, 2024, **8**, 385–394.
- 180 L. Petruzzi, T. Maier, P. Ertl and R. Hainberger, *Biosens. Bioelectron.: X*, 2022, **10**, 100136.
- 181 M. A. Rahman, R. K. Pal, N. Islam, R. Freeman, F. Berthiaume, A. Mazzeo and A. Ashraf, *Sensors*, 2023, **23**, 8115.
- 182 E. H. Yee, S. Lathwal, P. P. Shah and H. D. Sikes, *ACS Sens.*, 2017, **2**, 1589–1593.
- 183 C. Tortolini, V. Gigli, A. Angeloni, F. Tasca, N. T. K. Thanh and R. Antiochia, *Bioelectrochemistry*, 2024, **156**, 108590.
- 184 M. Zea, H. Ben Halima, R. Villa, I. A. Nemeir, N. Zine, A. Errachid and G. Gabriel, *Micromachines*, 2024, **15**, 1252.
- 185 S. Parween, D. S. P. and A. Asthana, *Sens. Actuators. B. Chem.*, 2019, **285**, 405–412.
- 186 Y. J. Lee, K. S. Eom, K.-S. Shin, J. Y. Kang and S. H. Lee, *Sens. Actuators. B. Chem.*, 2018, **271**, 73–81.
- 187 J. Lee, J. Song, J. Kim, A. Lee, S. Oh, B. Shin, K. Min and W.-H. Yeo, *Lab Chip*, 2026, **26**, 273–285.
- 188 E. L. Rossini, M. I. Milani, L. S. Lima and H. R. Pezza, *Spectrochim. Acta, Part A*, 2021, **248**, 119285.
- 189 J. Jaewjaroenwattana, W. Phoolcharoen, E. Pasomsub, P. Teengam and O. Chailapakul, *Talanta*, 2023, **251**, 123783.
- 190 J. Bhardwaj, A. Sharma and J. Jang, *Biosens. Bioelectron.*, 2019, **126**, 36–43.
- 191 A. N. Ramdzan, M. I. G. S. Almeida, M. J. McCullough and S. D. Kolev, *Anal. Chim. Acta*, 2016, **919**, 47–54.
- 192 C. Shende, C. Brouillette and S. Farquharson, *Analyst*, 2019, **144**, 5449.
- 193 C.-A. Bartlett, S. Taylor, C. Fernandez, C. Wanklyn, D. Burton, E. Enston, A. Raniczkowska, M. Black and L. Murphy, *Chem. Cent. J.*, 2016, **10**, 3.
- 194 T. S. M. Ferreira, R. B. R. Mesquita and A. O. S. S. Rangel, *Microchem. J.*, 2021, **11(11)**, 423.
- 195 H.-M. Wang, S.-Z. Lee and L.-M. Fu, *Micromachines*, 2026, **17**, 105.
- 196 R. S. Khan, Z. Khurshid and F. Y. I. Asiri, *Diagnostics*, 2017, **7**, 39.
- 197 T. Tian, H. Liu, L. Li, J. Yu, S. Ge, X. Song and M. Yan, *Sens. Actuators, B*, 2017, **251**, 440–445.
- 198 S. Hyung, G. Karima, K. Shin, K. S. Kim and J. W. Hong, *BioChip J.*, 2021, **15**, 252–259.
- 199 G. He, T. Dong, Z. Yang, A. Branstad, L. Huang and Z. Jiang, *Analyst*, 2022, **147**, 3305–3321.
- 200 C. Liu, D. Chu, K. Kalantar-Zadeh, J. George, H. A. Young and G. Liu, *Adv. Sci.*, 2021, **8**, 2004433.
- 201 N. Shakeeb, P. Varkey and A. Ajit, *Inflammation*, 2021, **44**, 1713–1723.
- 202 T. Diesch, C. Filippi, N. Fritschi, A. Filippi and N. Ritz, *Cytokine*, 2021, **143**, 155506.
- 203 Y. Lee, H. J. Park and J. H. Kim, *Biosens. Bioelectron.*, 2014, **57**, 208–214.
- 204 S. Bhaskar, S. Umrao, H. Lee, J. Tibbs, A. Bacon, S. Shepherd, T. Ayupova, F. U. Ciloglu, L. Liu, A. Tan, W.-C. Chen, M. T. T. Nguyen, M. G. Scannell, U. Aygun, U. Parlatan, C. Zhang, M. Kohli, G. R. Adami, W. Badar, R. C. Gaba, A. S. Mansfield, J. L. Schwartz, X. Wang, U. Demirci and B. T. Cunningham, *Lab Chip*, 2026, DOI: [10.1039/D5LC01014D](https://doi.org/10.1039/D5LC01014D).
- 205 S. Liu, Y. Hou, Z. Li, C. Yang and G. Liu, *ACS Sens.*, 2023, **8(9)**, 3520–3529.
- 206 L. A. Santana-Jiménez, A. Márquez-Lucero, V. Osuna, I. Estrada-Moreno and R. B. Dominguez, *Sensors*, 2018, **18**, 1071.
- 207 A. A. Bezerra Júnior, D. Pallos, J. R. Cortelli, C. H. C. Saraceni and C. S. Queiroz, *Revista Odonto Ciência*, 2010, **25**, 234–238.
- 208 L. E. B. Almeida, C. S. Machado, C. Dal-Fabbro, T. C. Chaves and C. M. de Felício, *J. Appl. Oral Sci.*, 2014, **22**, 165–170.
- 209 H.-H. Wan, H. Zhu, C.-C. Chiang, J.-S. Li, F. Ren, C.-T. Tsai, Y.-T. Liao, D. Neal, J. F. Esquivel-Upshaw and S. J. Pearton, *J. Vac. Sci. Technol., B*, 2024, **42**, 023202.
- 210 W. Ngwa, B. W. Addai, I. Adewole, V. Ainsworth, J. Alaro, O. I. Alatise, Z. Ali, B. O. Anderson, R. Anorlu, S. Avery, P. Barango, N. Bih, C. M. Booth, O. W. Brawley, J.-M. Dangou, L. Denny, J. Dent, S. N. C. Elmore, A. Elzawawy, D. Gashumba, J. Geel, K. Graef, S. Gupta, S.-M. Gueye, N. Hammad, L. Hessissen, A. M. Ilbawi, J. Kambugu, Z. Kozlakidis, S. Manga, L. Maree, S. I. Mohammed, S. Msadabwe, M. Mutebi, A. Nakaganda, N. Ndlovu, K. Ndoh, J. Ndumbalo, M. Ngoma, T. Ngoma, C. Ntizimira, T. R. Rebbeck, L. Renner, A. Romanoff, F. Rubagumya, S. Sayed, S. Sud, H. Simonds, R. Sullivan, W. Swanson, V. Vanderpuye, B. Wiafe and D. Kerr, *Lancet Oncol.*, 2022, **23**, e251–e312.
- 211 K. Permpoka, P. Purinai, C. Cheerasiri, W. Rojpalakorn, V. Nilaratanakul and W. Laiwattanapaisal, *Sens. Actuators. B. Chem.*, 2024, **398**, 134712.
- 212 V. Bianchi, A. Boni, M. Bassoli, M. Giannetto, S. Fortunati, M. Careri and I. De Munari, *IEEE Access*, 2021, **9**, 141544–141554.
- 213 P. P. E. Campos, H. A. Silva-Neto, L. C. Duarte, J. F. S. Petrucci and W. K. T. Coltro, *Anal. Chem.*, 2025, **97**, 15818–15825.
- 214 A. A. Rowe, A. J. Bonham, R. J. White, M. P. Zimmer, R. J. Yadgar, T. M. Hobza, J. W. Honea, I. Ben-Yaacov and K. W. Plaxco, *PLoS One*, 2011, **6**, e23783.
- 215 S. C.-H. Lee and P. J. Burke, *Electrochim. Acta*, 2022, **422**, 140481.
- 216 Z. H. Ning, J. Q. Huang, S. X. Guo and L. H. Wang, *J. Phys. Conf. Ser.*, 2020, **1550**, 042049.

- 217 C. Ferreira, F. Barry, M. Todorović, P. Sugrue, S. R. Teixeira and P. Galvin, *Sensors*, 2025, **25**, 762.
- 218 I. Anshori, I. F. Ramadhan, E. Ariasena, R. Siburian, J. Affi, M. Handayani, H. Yunkins, T. Kuji, T. L. E. R. Mengko and S. Harimurti, *IEEE Access*, 2022, **10**, 112578–112593.
- 219 Y.-L. Wang and C.-M. Cheng, *Microfluid. Nanofluid.*, 2026, **30**, 15.
- 220 S. K. Sailapu, S. Liébana, I. Merino-Jimenez, J. P. Esquivel and N. Sabaté, *Biosens. Bioelectron.*, 2024, **243**, 115708.
- 221 N. H. Bhuiyan, M. J. Uddin, J. Lee, J. H. Hong and J. S. Shim, *Adv. Mater. Technol.*, 2022, **7**, 2101690.
- 222 D. Solano and S. Camacho-Leon, *Microsyst. Technol.*, 2025, **31**, 1289–1301.
- 223 V. Galstyan, I. D'Onofrio, A. Liboà, G. De Giorgio, D. Vurro, L. Rovati, G. Tarabella and P. D'Angelo, *Adv. Mater. Technol.*, 2024, **9**, 2400395.
- 224 E. Cho, M. Mohammadifar and S. Choi, *Micromachines*, 2017, **8**, 265.
- 225 C. Fischer, A. Fraiwan and S. Choi, *Biosens. Bioelectron.*, 2016, **79**, 193–197.
- 226 A. Pal, H. E. Cuellar, R. Kuang, H. F. N. Caurin, D. Goswami and R. V. Martinez, *Adv. Mater. Technol.*, 2017, **2**, 1700130.
- 227 M. Mohammadifar and S. Choi, *Adv. Mater. Technol.*, 2017, **2**, 1700127.
- 228 M. Parrilla, A. Vanhooydonck, R. Watts and K. De Wael, *Biosens. Bioelectron.*, 2022, **197**, 113764.
- 229 T. Arakawa, K. Tomoto, H. Nitta, K. Toma, S. Takeuchi, T. Sekita, S. Minakuchi and K. Mitsubayashi, *Anal. Chem.*, 2020, **92**, 12201–12207.
- 230 X. Chen, J. Lan, Y. Liu, L. Li, L. Yan, Y. Xia, F. Wu, C. Li, S. Li and J. Chen, *Biosens. Bioelectron.*, 2018, **102**, 582–588.
- 231 B. Chutvirasakul, N. Nuchtavorn, L. Suntornsuk and Y. Zeng, *Electrophoresis*, 2020, **41**, 311–318.
- 232 S. Guo, H. Xie, X. Zhao, H. He, X. Feng, Y. Li, B. Liu and P. Chen, *Analyst*, 2024, **149**, 1250–1261.